Fermi National Accelerator Laboratory

FERMILAB-FN-678

Beam Instability Issues of the 50 GeV x 50 GeV Muon Collider Ring

K.Y. Ng

Fermi National Accelerator Laboratory
P.O. Box 500, Batavia, Illinois 60510

June 1999

Operated by Universities Research Association Inc. under Contract No. DE-AC02-76CH03000 with the United States Department of Energy

FN-678

BEAM INSTABILITY ISSUES OF THE 50 GEV × 50 GEV MUON COLLIDER RING

King-Yuen Ng

Fermi National Accelerator Laboratory, P.O. Box 500, Batavia, IL 60510*

(March 1999)
(Final Version, September 1999)

Abstract

Single bunch instabilities for the 50 GeV × 50 GeV muon collider are discussed. An impedance budget of the collider is estimated. A phase-slip factor of $|\eta| = 1 \times 10^{-6}$ is desired to avoid excessive rf systems. Potential-well distortion of a smooth bunch can be compensated by rf cavities. Accumulated growth in energy due to imperfections and noises in the muon bunch can be reduced by smoothing the bunch distribution before injection. The growth due longitudinal microwave instability is small because of the compensated rf cavities, the finite lifetime of the muons, and the choice of a small $|\eta|$. Beamloadings in the compensating rf cavities are large and suitable feed-forward cancellation is required. Transverse microwave instability can be damped by chromaticities and octupoles. Beam breakup can be cured by Balakin-Novokhatsky-Smirnov damping in principle, but is nontrivial in practice. When beam breakup is small, it can possibly be damped by a betatron tune spread in the beam.

*Operated by the Universities Research Association, Inc., under contract with the U.S. Department of Energy.

I. INTRODUCTION

Muon colliders offer significant advantage in the production of Higgs bosons over electron colliders. This is because the muon mass is $m_\mu/m_e = 105.7/0.5110 = 206.8$ times larger than the electron mass, so that the production cross section is $m_\mu^2/m_e^2 = 4.28 \times 10^4$ times larger. Therefore, very probably, the first muon collider to be built will be 50 GeV on 50 GeV, through which light Higgs bosons having masses around 100 GeV/c^2 can be produced. In order to attain the luminosity of 1×10^{32} cm^{-2}s^{-1} for the accumulation of 1.9×10^3 Higgs bosons in a year, each of the colliding μ^+ and μ^- bunches needs to have an intensity of $N = 4\times10^{12}$ particles, rms bunch length $\sigma_\ell = 4$ cm, and rms momentum spread $\sigma_\delta = 1.2\times10^{-3}$ [1]. Unlike electron colliders, beamstrahlung is not a problem in the muon interaction region; it is possible to have the momentum spread of the muon beams to be as small as $\sigma_\delta = 3.0 \times 10^{-5}$. As a result, there is another mode of operation of the muon collider at this small momentum spread with rms bunch length $\sigma_\ell = 13$ cm for the precision determination of the Higgs boson mass. With such a high-intensity bunch and small momentum spreads, the study of beam instabilities becomes a very important task.

II. IMPEDANCE BUDGET

Without detailed design of the collider ring, it is difficult to compute the coupling impedances of the vacuum chamber. Nevertheless, an estimate is possible.

A. BEAM PIPE RADIUS

The muon collider ring has to be as small as possible so that there will be more collisions between the positive and negative muon bunches before the muons decay appreciably. As a result, superconducting magnets, which have higher pole-tip magnetic flux density are used. To prevent the decay products from the muons from quenching the superconducting windings, the magnets are lined with a tungsten shielding having a thickness of about 3.5 cm. Thus the physical aperture of the colliding ring will not be large. For example, a quadrupole in the arc of the ring has a magnetic flux density gradient of about 130 T/m. If the quadrupole aperture is 6 cm so that the physical aperture at the shielding is only 2.5 cm, the pole-tip magnetic flux density reaches 7.8 T already.

The collider lattice designed by Trbojevic and Ng [1] has a circumference of roughly $C = 2\pi R = 350$ m. One half of the ring consists of the interacting region with focusing triplets, where the betatron functions reach 1550 m, and the local chromaticity correction

regions, where the betatron functions reach 100 m. The other half of the ring consists of arcs and a long straight section, where the maximum horizontal and vertical betatron functions are 19.57 m and 23.63 m, respectively, while the dispersion varies between -3.5 and $+1.5$ m. There is also another better optimized version of the same lattice having dispersion between -2.9 and $+1.5$ m, which we will use in this discussion. The rms $\sigma_\ell = 13$ cm bunch with rms momentum spread $\sigma_\delta = 3 \times 10^{-5}$ has a normalized rms emittance of 290×10^{-6} πm in both the horizontal and transverse directions. Thus, the rms bunch radius is 3.81 mm in the horizontal direction and smaller in the vertical. On the other hand, the rms $\sigma_\ell = 4$ cm bunch with rms momentum spread $\sigma_\delta = 1.2 \times 10^{-3}$ has a normalized rms emittance of 85×10^{-6} πm. Taking into account of the dispersion, the horizontal rms bunch radius is therefore 3.93 mm and smaller in the vertical. Assuming an aperture of 5σ, the beam-pipe radius in the arcs and long straight section can be set at $b = 2$ cm. For the other half of the ring, we can take the average betatron function to be 100 m, and the average beam-pipe radius can be set at $b = 4$ cm.

B. BEAM-POSITION MONITORS

Because of the limited physical aperture of the colliding ring, careful beam monitoring becomes essential. Assume strip-line beam-position monitors (BPMs) like those of the Fermilab Tevatron are installed. Each BPM consists of 2 cylindrical strip-lines of radius b, each subtending a full angle ϕ_0 at the center of the beam pipe and of length ℓ. Each strip-line forms a transmission line of characteristic impedance $Z_c = 50$ Ω with the beam-pipe wall that bulges out, and is terminated at both ends by the resistors Z_c to prevent resonances. The longitudinal and transverse coupling impedances have been calculated to be [2]

$$Z_\parallel = 2MZ_c \left(\frac{\phi_0}{2\pi}\right)^2 \left(\sin^2\frac{\omega\ell}{c} + j\sin\frac{\omega\ell}{c}\cos\frac{\omega\ell}{c}\right) , \tag{2.1}$$

$$Z_\perp = \frac{c}{b^2}\left(\frac{4}{\phi_0}\right)^2 \sin^2\frac{\phi_0}{2}\,\frac{Z_\parallel}{\omega}\,F_{\rm H,V} , \tag{2.2}$$

where $F_{\rm H}$ and $F_{\rm V}$ are the fractions of sets of BPMs, respectively, for the horizontal and vertical, since each set of BPM strip-lines can work only for either the horizontal or the vertical. At low frequencies, the impedances are inductive,

$$\frac{Z_\parallel}{n} = j2MZ_c\left[\frac{\phi_0}{2\pi}\right]^2 \frac{\ell}{R} , \tag{2.3}$$

$$Z_\perp = \left[\frac{4}{\phi_0}\right]^2 \frac{R}{2b^2}\sin^2\frac{\phi_0}{2}\left[\frac{Z_\parallel}{n}\right] . \tag{2.4}$$

At high frequencies, the reactive parts of the impedances oscillate between inductive and capacitive; for example, the first zero occurs at frequency $f = c/(2\ell) = 1.50$ GHz, where the length of the strip-line is assumed to be $\ell = 10$ cm. The real parts rise from zero quadratically with frequency for $Z_\parallel$ and linearly for $Z_\perp$, peak at 1.50 GHz, and oscillate afterwards.

Note that these impedances are roughly independent of the circumference of the collider ring, because more BPMs will be needed for a larger ring. The betatron tunes are roughly $\nu_\beta = 8.13$ in the horizontal and 6.24 in the vertical. To correct the orbit, one needs about 4 BPMs per betatron wavelength. Therefore, we are going to use $M = 56$ pairs of strip lines, 32 for the horizontal and 24 for the vertical, or $F_H = 32/56$ and $F_V = 24/56$. In the Tevatron, each BPM has a length of $\ell = 18$ cm and a full subtending angle $\phi_0 = 110°$. Here, the bunch lengths are relatively shorter than the Tevatron bunches which have rms length ~ 16 cm. Thus, we use 10-cm strip-lines instead. Also the intensity of a Tevatron bunch is around 5×10^{11} particles, much weaker than that of the muon bunches. We therefore imagine that strip-lines with smaller subtending angle, for example $\phi_0 = 75°$, will be able to pickup enough beam signals for orbit monitoring. With these BPMs parameters, we obtain $Z_\parallel/n = j0.44\ \Omega$ and $Z_\perp = j0.075$ and $j0.056$ MΩ/m, respectively, for the horizontal and vertical BPMs. In computing the transverse impedance, we have assumed that the strip-line radius is $b = 2$ cm for half of the ring and $b = 4$ cm for the other half. It is worthwhile to point out that, while the transverse impedance is inversely proportional to the square of the strip-line radius, the longitudinal impedance is independent of the strip-line radius.

C. BELLOWS

The impedances of the bellows are roughly proportional to the ring circumference. For the Tevatron, which has a circumference of 6.28 km, the contributions at low frequencies are $Z_\parallel/n \sim j0.4\ \Omega$ and $Z_\perp \sim j0.4$ MΩ/m [3]. The 50 GeV$\times$50 GEV muon collider is about 18 times smaller. However, there are many more elements per unit length in the muon colliders. Here, we scale the impedances by a factor of 10 instead to get $Z_\parallel/n \sim j0.04\ \Omega$ and $Z_\perp \sim j0.04$ MΩ/m. We like to point out that a beam-pipe radius of $b \approx 4$ cm has been used in the Tevatron. Here, the beam pipe radius is smaller. As a result, the impedances may be larger and extend out to higher frequencies.

The Tevatron bellows are unshielded. We do hope that these impedances would be much smaller if the bellows in the muon collider were shielded. However, in the electron-positron colliding ring LEP at CERN, the bellows, although shielded, still contribute roughly 40% to the longitudinal coupling impedance when the rms bunch length is 1 cm [4]. Therefore,

it is unclear how much the shielded bellows in the muon collider will contribute to the longitudinal and transverse coupling impedances. Careful design of the shielded bellows and more detailed computation are required to answer this question.

D. RESISTIVE WALL

For the resistive walls of the vacuum chamber, the contributions to the impedances are

$$\frac{Z_\parallel}{n} = \frac{\mathrm{sgn}(n) + j}{2b} \left[\frac{Z_0 \rho C}{\pi |n|}\right]^{1/2} , \tag{2.5}$$

$$Z_\perp = \frac{C}{\pi b^2} \left[\frac{Z_\parallel}{n}\right] , \tag{2.6}$$

where $Z_\perp$ is to be evaluated at $n+\nu_\beta$, ν_β is the betatron tune, and n the revolution harmonic. For an aluminum beam pipe with resistivity $\rho = 0.0265$ $\mu\Omega$-m, we obtain

$$\frac{Z_\parallel}{n} = [\mathrm{sgn}(n) + j] 0.62 |n|^{-1/2} \, \Omega , \tag{2.7}$$

$$Z_\perp = [\mathrm{sgn}(n) + j] 0.13 |n + \nu_\beta|^{-1/2} \, \mathrm{M}\Omega/\mathrm{m} , \tag{2.8}$$

using $b = 2$ and 4 cm for each half of the ring. Thus, at the beam-pipe cutoff frequency, $f_c = 2.405c/(2\pi b) = 5.74$ GHz, c being the velocity of light, the resistive-wall contributions become negligibly small compared with the contributions of the BPMs.

E. BROADBAND IMPEDANCE MODEL

For the injection of the positive muon bunch and negative muon bunch, we will need at least two Lambertson magnets and two kickers, which will usually have significant contributions to the coupling impedances. Also there is a big variation of betatron functions around the ring, resulting in many transitions in the cross section of the vacuum chamber. These transitions will also have significant contributions to the coupling impedances.

Without detailed knowledge of the vacuum chamber, it will be advisable to assume a broadband impedance model for the ring, or

$$Z_\parallel = \frac{R_\parallel}{1 - jQ\left(\frac{\omega_r}{\omega} - \frac{\omega}{\omega_r}\right)} , \tag{2.9}$$

$$Z_\perp = \frac{c}{\omega} \frac{R_\perp}{1 - jQ\left(\frac{\omega_r}{\omega} - \frac{\omega}{\omega_r}\right)} . \tag{2.10}$$

Here, we choose the quality factor $Q = 1$ and the angular resonant frequency $\omega_r = 50$ GHz (or $f_r = 7.96$ GHz) for both the longitudinal and transverse. The resonant frequency is about 38% higher than the cutoff frequency f_c for a 2 cm radius circular beam pipe. We choose a higher resonant frequency because we are aware that in both the damping rings at SLAC and the electron-positron colliding ring LEP at CERN, when detailed small high-frequency contributions are added up, $Z_\parallel/n$ does not roll off even at frequency $f = 10$ GHz (or $\omega = 63$ GHz) [5]. From the analysis above, we choose here the shunt impedances $R_\parallel$ and $R_\perp$ so that $Z_\parallel/n = 0.5\,\Omega$ and $Z_\perp = 0.1\,\mathrm{M}\Omega/\mathrm{m}$ at the angular resonant frequency. Then, we also have $\mathcal{I}m\, Z_\parallel/n = 0.5\,\Omega$ and $\mathcal{I}m\, Z_\perp = 0.1\,\mathrm{M}\Omega/\mathrm{m}$ at lower frequencies. We believe that it will be difficult to make the impedances smaller than these values in such a small ring.

III. PHASE-SLIP FACTOR

Longitudinally, the worst fast collective growth is usually the microwave instability. The Boussard-modified Keil-Schnell stability criterion for a Gaussian distributed bunch is [6]

$$\left|\frac{Z_\parallel}{n}\right| \le \frac{2\pi|\eta|E\sigma_\delta^2}{eI_{\rm pk}} \ , \tag{3.1}$$

where η is the phase-slip factor, $I_{\rm pk}$ is the peak current, E the muon energy, and e its charge. Taking the $\sigma_\ell = 4$ cm bunch with $\sigma_\delta = 1.2 \times 10^{-3}$, stability can be assured only if $|\eta| > 0.00212$. Neglecting the influence of coupling impedance, to keep such a bunch in an rf bucket, the synchrotron tune will be

$$\nu_s = \frac{|\eta|R\sigma_\delta}{2\pi\sigma_\ell} = 3.54 \times 10^{-3} \ . \tag{3.2}$$

Assuming that the bucket height will be $k = 5$ times the rms momentum spread of the bunch, the rf harmonic is

$$h = \left[\frac{C}{\pi k\sigma_\ell}\right]_{\rm integer} = 557 \ . \tag{3.3}$$

Thus, the rf voltage will be

$$V_{\rm rf} = \frac{2\pi E\nu_s^2}{h|\eta|} = 3.34 \text{ MV} \ , \tag{3.4}$$

which is very large, and will be much larger when the longitudinal impedance is included. Another choice of operation is to make $|\eta|$ as small as possible. Although we have to give up Landau damping, hopefully, the growth rate, which is proportional to $\sqrt{|\eta|}$, may be slow enough and cause insignificant harm. Here, we are talking about the total spread in η, since

the latter is a function of momentum spread δ. The phase-slip factor η that records the slip in revolution period T from the on-momentum revolution period T_0 can be expanded as

$$\frac{\Delta T}{T_0} = \eta\delta = \eta_0\delta + \eta_1\delta^2 + \eta_2\delta^3 + \cdots \quad . \tag{3.5}$$

On the other hand, the length of the closed orbit C is also a function of the momentum spread, and can be expanded around the length of the on-momentum orbit C_0 according to

$$C = C_0(1 + \alpha_0\delta + \alpha_1\delta^2 + \alpha_2\delta^3 + \cdots) \ , \tag{3.6}$$

where α_i is the i-th order of the momentum compaction. It is then not difficult to obtain

$$\eta_0 = \alpha_0 - \frac{1}{\gamma^2} \ , \quad \eta_1 = \alpha_1 - \frac{\eta_0}{\gamma^2} + \frac{3\beta^2}{2\gamma^2} \ , \quad \eta_2 = \alpha_2 - \frac{\eta_1}{\gamma^2} + \frac{3\beta^2\eta_0}{2\gamma^2} + \frac{(1-5\beta^2)\beta^2}{2\gamma^2} \ , \ \cdots \ , \tag{3.7}$$

where $\gamma = 472.223$ and $\beta = \sqrt{1-1/\gamma^2}$ are the relativistic Lorentz factors of the on-momentum 50 GeV muons. To reduce the spread in η up to about $3\sigma_\delta$, we need to control the contribution of the higher-order momentum compaction also. The first-order effect of sextupoles controls η_1, the first-order effect of octupoles controls η_2, etc. The experience with the 2 TeV×-2 TeV muon collider lattice [7] indicates that we need to control up to the contribution of η_2 and that it will be rather hard to reduce the spread of $|\eta|$ to below 1×10^{-6}. As a result, this value of $|\eta|$ will be used in our discussion below. In fact, as will be clear later, an $|\eta|$ smaller than 1×10^{-6} will not help in lowering the growth of the energy spread of the muon bunch. A particle at an energy spread of $3\sigma_\delta$ in the 4-cm bunch will drift by 4.2 ps (0.13 cm) only in 1000 turns. Note that the muons have a e-folding lifetime of $\tau_0 = 2.19703$ μs at rest. At 50 GeV, however, the e-folding lifetime is $\tau = \gamma\tau_0 = 1039.69$ μs or $n_\tau = 890.542$ turns in a ring of circumference 350 m. Therefore, we only care about roughly the first 1000 turns after the muon bunches are injected into the collider ring. This is another reason why such a small $|\eta|$ is used, because no bunching rf will be necessary. However, this is not true in the presence of the longitudinal coupling impedance.

IV. POTENTIAL-WELL DISTORTION AND MICROWAVE INSTABILITY

A. WAKE POTENTIAL COMPENSATION

Particles in the high-intensity bunch will be affected by the wake from the particles ahead. Assume a linear Gaussian distribution for the bunch and a broadband impedance

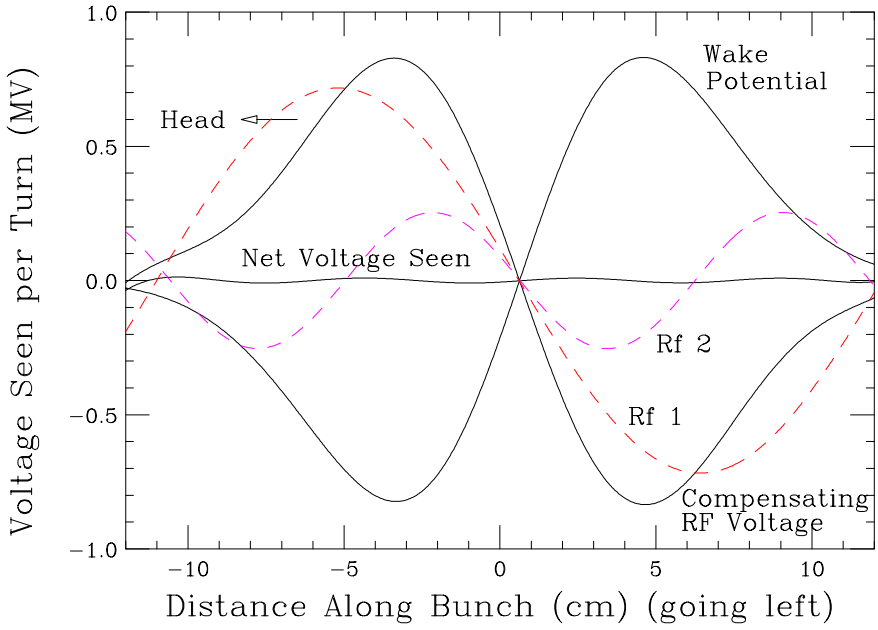

Figure 1: (color) Wake potential, compensating rf voltages, and net voltage seen by particles in the 4-cm bunch at injection. The compensating rf is the sum of two rf's represented by red and magenta dashes.

for the vacuum chamber with $Q = 1$ and $Z_\parallel/n = 0.5\ \Omega$ at the angular resonant frequency $\omega_r = 50$ GHz. The wake function at a distance z behind a unit source charge is

$$W_0(z) = -\frac{\omega_r R_\parallel}{Q}\, e^{-\alpha z/c}\left[\cos\frac{\bar{\omega} z}{c} - \frac{\alpha}{\bar{\omega}}\sin\frac{\bar{\omega} z}{c}\right] , \tag{4.1}$$

where $R_\parallel = n_r\, \mathcal{R}e\, Z_\parallel/n$ is the shunt impedance or the impedance at the resonant harmonic n_r or angular resonant frequency ω_r as given by Eq. (2.9), $\alpha = \omega_r/(2Q)$ is the damping rate of the wake, $\bar{\omega} = \sqrt{\omega_r^2 - \alpha^2}$ is the shifted resonant angular frequency, and the particle velocity has been taken as c. The wake potential seen by a particle inside a Gaussian bunch of rms length σ_ℓ at a distance z behind the bunch center is

$$V(z) = e\int_{-\infty}^{z} dz'\rho(z')W_0(z - z') , \tag{4.2}$$

where $\rho(z)$ is the bunch distribution. The integration gives

$$V(z) = -\frac{eN\omega_r R_\parallel}{2Q\cos\phi_0}\,\mathcal{R}e\; e^{j\phi_0 - z^2/(2\sigma_\ell^2)} w\left[\frac{\sigma_\ell\omega_r e^{j\phi_0}}{c\sqrt{2}} - \frac{jz}{\sqrt{2}\sigma_\ell}\right] , \tag{4.3}$$

where N is the total number of particles in the bunch, $\sin\phi_0 = 1/(2Q)$, and w is the complex error function.

At such a high resonant frequency, the wake potential seen by a bunch particle is roughly equal to the derivative of the Gaussian with a maximum and minimum of $\Delta E_0 \sim \pm 0.83$ MV, as shown in Fig. 1. Therefore, taking into account the reduction in intensity due to the decay of the muon, some particles will gain and some will lose in $n_f = 1000$ turns as much as

$$\Delta E = \Delta E_0 \int_0^{n_f} e^{-n/n_\tau} dn = \Delta E_0 \, n_\tau \left(1 - e^{-n_f/n_\tau}\right) = 499 \text{ MeV} \ , \tag{4.4}$$

where $n_\tau = \gamma \tau_0 f_0 = 890.542$ is the e-folding lifetime in turns of the 50 GeV muons in the collider ring, with $n_{\rm eq} = n_\tau \left(1 - e^{-n_f/n_\tau}\right) = 601$ serving conveniently as an equivalent number of turns in the presence of the muon decay. On the other hand, the designed rms energy spread is only 60 MeV. With such a large energy spread, there will be some drift in time, especially in the situation when a larger $|\eta|$ is used. Thus, there may be bunch lengthening as well as particle loss due to the limited physical aperture of the vacuum chamber. Kim, Wurtele, and Sessler [8] suggested to compensate this incoherent energy change by using rf voltages. If the linear distribution is parabolic, a sinusoidal rf of wavelength longer than the bunch length will compensate for this bunch distortion due to the wake potential. If the linear distribution is cosine-square, a sinusoidal rf with wavelength exactly equal to the bunch length will do the job. For a Gaussian distribution, one needs a combination of sinusoids. A beam particle at a distance z behind the bunch center should see the rf voltage

$$V_{\rm rf}(z) = \sum_{i=1}^{n} V_i \sin\left(\frac{\omega_i z}{c} + \varphi_i\right) \ . \tag{4.5}$$

For example, we try to use two rf's to compensate up to $\pm 3\sigma_\ell$ of the bunch. At injection of the 4-cm bunch, the optimum parameters are, for frequencies $\omega_1/(2\pi) = 1.290$ GHz and $\omega_2/(2\pi) = 2.673$ GHz, for voltages $V_1 = 717.4$ kV and $V_2 = 253.4$ kV, and for phases $\varphi_1 = 170.55^\circ$ and $\varphi_2 = 159.33^\circ$, as shown in Fig. 1. These rf voltages have to decrease turn by turn according to the decay of the muons. Note that the compensation rf frequencies are not completely free parameters for optimization; they have to be harmonics of the revolution frequency. Tracking was done for 1000 turns using 2×10^6 macro-particles, populated randomly according to a bi-Gaussian distribution in the longitudinal phase space. The tracking code is a variation of TRISIM developed by Sabbi [9], where triangular bins are used. The half triangular bin width is $w_b = 15$ ps (0.45 cm) which is fine enough for resonant frequency up to $f_r = 1/(2w_b) = 33$ GHz or $\omega_r = 209$ GHz. Such narrow bin width is required because we must have reasonable number of bins for $\sim \pm 3\sigma_\ell$ to represent the bunch. Near the center of the bunch, the number of macro-particles per bin is $\sim 80,000$ (and $\sim 28,000$ for the 13-cm bunch). The tracking result for 1000 turns is shown in Fig. 2. We see that the compensation rf's do a good job by keeping the muons bunched without any increase in bunch length. It

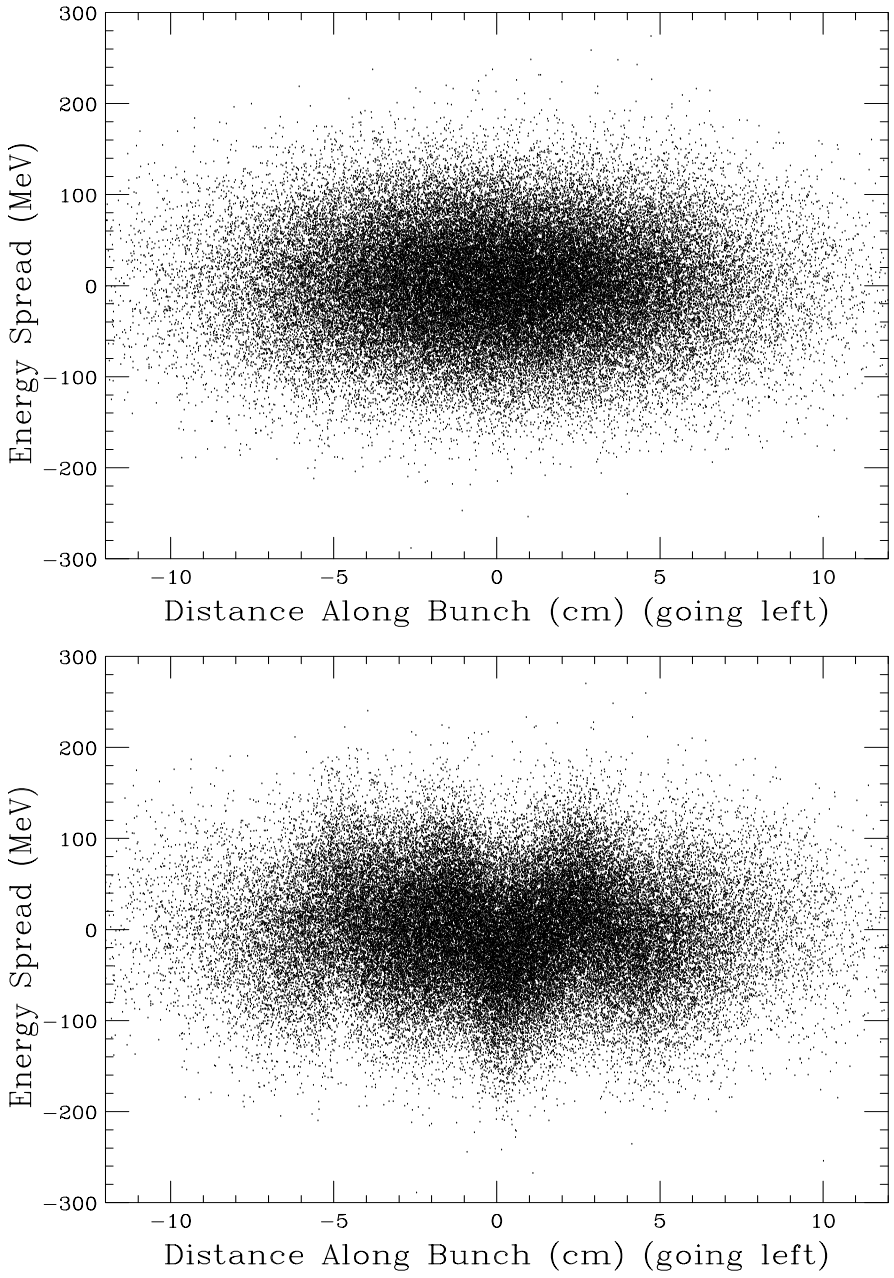

Figure 2: Simulation of the 4-cm bunch of 4×10^{12} muons subject to a broadband impedance with quality factor $Q = 1$ and $Z_\parallel/n = 0.5\ \Omega$ at the resonant angular frequency $\omega_r = 50$ GHz. The half-triangular bin width is 15 ps (0.45 cm) and 2×10^6 macro-particles are used. Top plot shows initial distribution with $\sigma_E = 60$ MeV and $\sigma_\ell = 4$ cm. Lower plot shows distribution after 1000 turns with compensating rf's initially at $\omega_1/(2\pi) = 1.290$ GHz and $\omega_2/(2\pi) = 2.673$ GHz, voltages $V_1 = 717.4$ kV and $V_2 = 253.4$ kV, and phases $\varphi_1 = 170.55°$ and $\varphi_2 = 159.33°$. The rf voltages decrease according to the decay of the muons.

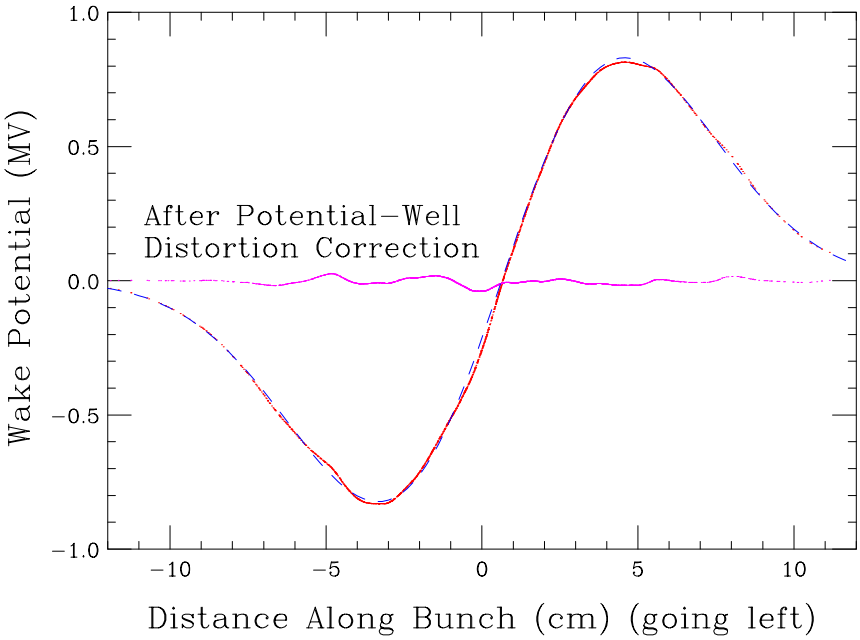

Figure 3: (color) Wake potential seen by the simulated bunch is shown by the red curve, which differs slightly from the wake potential of an ideal smooth Gaussian bunch shown in blue dashes. The difference shown by the magenta solid curve represents the random fluctuation of the finite number of macro-particles.

is important to point out that this rf compensation only compensates the wake potential between $\pm 3\sigma_\ell$ of the bunch. Particles outside this region will acquire large energy increase or decrease and will probably be lost. However, this loss represents only about 0.27% of the beam particles. Compensation to more than $3\sigma_\ell$ is definitely possible, if, for example, rf's with 3 or more frequencies are used.

Coming back to Fig. 2, we see some ripples along the bunch. They are not due to inexact compensation of the theoretical wake potential, because Fig. 1 shows that the net voltage seen has ripples with wavelength about 210 ps and $\sim \pm 0.008$ MV at injection or $\sim \pm 4.8$ MV for 1000 turns. On the other hand, Fig. 2 shows ripples of $\sim \pm 40$ MeV with wavelength of ~ 125 ps, corresponding to the resonant frequency of the impedance. These ripples actually come from the deviation of the actual bunch distribution from being exactly Gaussian. Figure 3 shows the wake potential of the simulated bunch in the solid red curve. We see that it differs from the ideal wake potential curve of a smooth Gaussian bunch shown by blue dashes. The difference is the magenta solid curve. It is these fluctuations that give rise to the ripples in the bunch after 1000 turns. This clearly illustrates that the rf's can only compensate for potential-well distortion for a smooth bunch and *cannot* cope with a bunch

Table I: Two-sinusoidal fits for potential-well compensation.

	V_i (kV)	harmonic	f_i (GHz)	φ_i (rad)
4-cm bunch	717.4	1506	1.290	2.9767
	253.4	3249	2.673	2.7808
13-cm bunch	65.40	445	0.3854	3.0927
	24.74	930	0.7966	3.0418

having imperfections or noises. It is worthwhile to point out that although the statistical particle fluctuations near the center of the bunch are $\sim 0.35\%$, the magenta curve in Fig. 3 shows much larger fluctuations. This is because the wake function for a point charge is approximately the same as the derivative of a delta-like function having a width of the order the wavelength of the resonant frequency of the impedance. In other words, the magenta curve shows the *slopes* of the statistical particle fluctuations. This also explains why the fluctuations have roughly the same frequency of the impedance. In reality, the impedance of the ring is never an ideal broadband; it may contain, for example, other sharp and broad resonances. All these deviations from the broadband impedance should also show up as the residual wake in the magenta curve of Fig. 3 for a real collider ring.

For the 13-cm bunch, the wake potential of the ideal smooth Gaussian is shown in Fig. 4 together with the sum of the compensation rf's, which at injection are at $\omega_1/(2\pi) = 0.3854$ GHz and $\omega_2/(2\pi) = 0.7966$ GHz, with $V_1 = 65.40$ kV and $V_2 = 24.74$ kV, and $\varphi_1 = 177.20^\circ$ and $\varphi_2 = 174.28^\circ$. These numbers are listed in Table I for the two bunches.

Figure 5 shows initial particle distribution of the 13-cm bunch which has a rms energy spread of 1.5 MeV. The lower plot shows the simulation result after 1000 turns with the compensating rf's turned on and with the rf voltages reducing according to the decay of the muons. We see that the momentum distribution is around ± 10 MeV, about $\pm 7\sigma_\delta$, and is definitely too large to be acceptable. Here, we use the same number of macro-particles, the same bin width, and the same broadband impedance as in the situation of the 4-cm bunch. The deviation of the wake potential of the simulated bunch from that of the ideal smooth Gaussian bunch is shown in Fig. 6. Again, the fluctuations are due to the finite number of randomly Gaussian-distributed macro-particles. In Ref. [8], this growth of momentum spread corresponding to the resonant frequency of the impedance is not seen in any of the simulations, although a much smaller number of macro-particles were used there. One of the reasons is that the macro-particles were *quietly* populated rather than randomly, thus smoothing out all the energy jitters or seeds for any growth development. The other reason

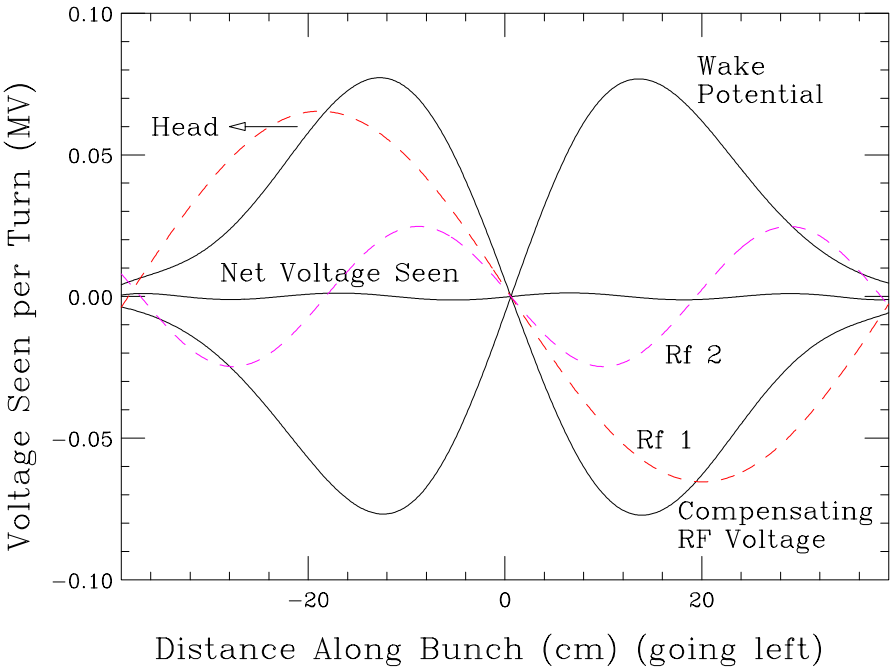

Figure 4: (color) Wake potential, compensating rf voltages, and net voltage seen by particles in the 13-cm bunch at injection. The compensating rf is the sum of two rf's represented by red and magenta dashes.

comes from the fact that a much smaller longitudinal impedance, $Z_\parallel/n = 0.1\ \Omega$ at resonant angular frequency $\omega_r = 10$ GHz, had been used, thus slowing the growths.

It appears from Figs. 2 and 5 that the accumulated growth in energy spread is much worse for the 13-cm bunch than the 4-cm bunch. In fact, this is not true. For the 4-cm bunch, the growth is about ± 160 MeV after 1000 turns. But the initial rms energy spread is 60 MeV. Taking the original spread to be 2σ, the actual accumulated growth is actually about ± 40 MeV. On the other hand, the growth for the 13-cm bunch is ± 10 MeV. But the initial rms energy spread is only 1.5 MeV. Thus, the actual growth is only about ± 7 MeV after subtracting 2σ. In fact, we have been using the same bin size and the same number of macro-particles in the two simulations. Thus, the statistical particle fluctuations or seed will be $\sqrt{13/4}$ larger for the 13-cm bunch. Otherwise the growth would have been only $\sqrt{4/13}\times 7 = 3.9$ MeV instead. However, relative to its initial energy spread, the accumulated energy growth of the 4-cm bunch is not large and is acceptable, while that for the 13-cm bunch is too large and is not acceptable.

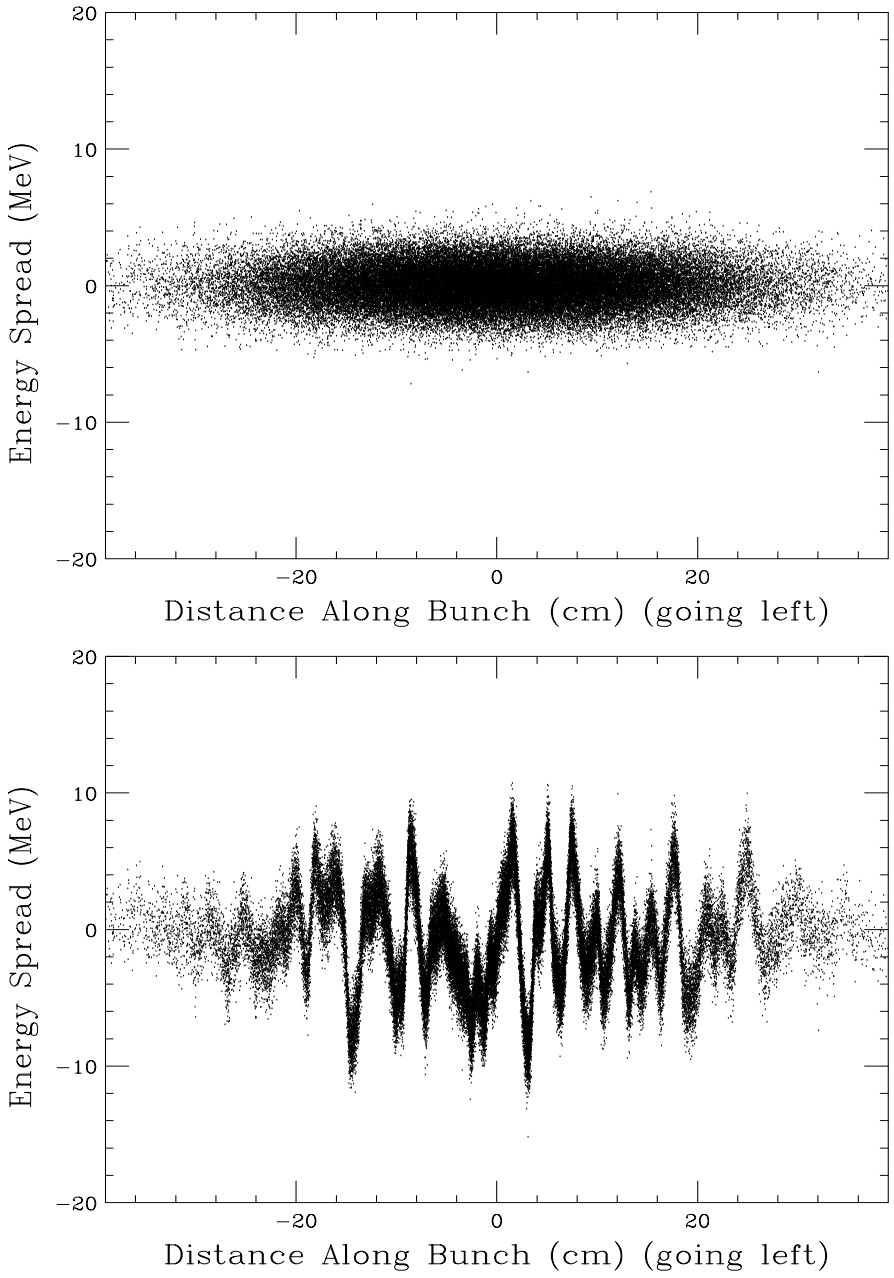

Figure 5: Simulation of the 13-cm bunch of 4×10^{12} muons subject to a broadband impedance with quality factor $Q=1$ and $Z_\parallel/n=0.5\ \Omega$ at the resonant angular frequency $\omega_r=50$ GHz. The half-triangular bin width is 15 ps (0.45 cm) and 2×10^6 macro-particles are used. Top plot shows initial distribution with $\sigma_E=1.5$ MeV and $\sigma_\ell=13$ cm. Lower plot shows distribution after 1000 turns with compensating rf's initially at $\omega_1/(2\pi)=0.3854$ GHz and $\omega_2/(2\pi)=0.7966$ GHz, voltages $V_1=65.40$ kV and $V_2=24.74$ kV, and phases $\varphi_1=177.20°$ and $\varphi_2=174.28°$. The rf voltages decrease according to the decay of the muons.

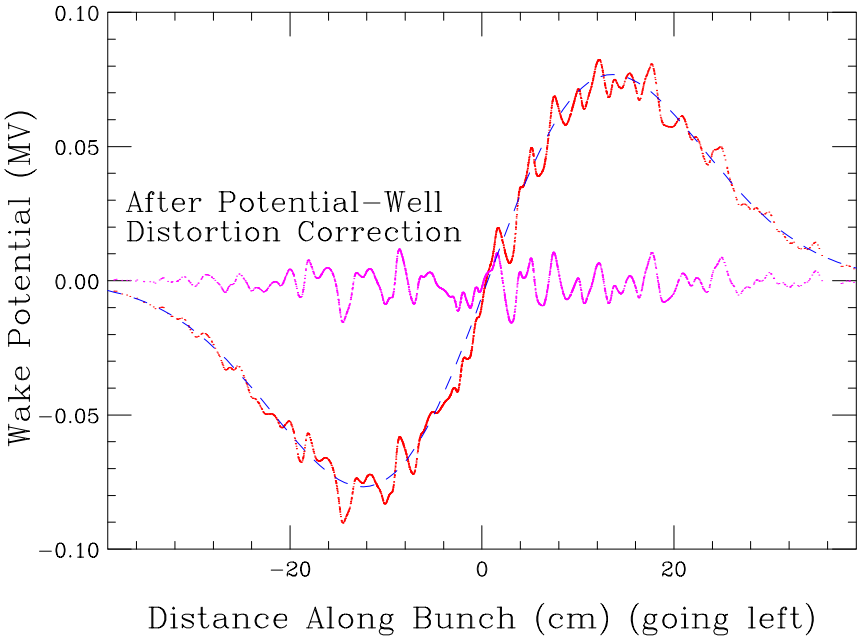

Figure 6: (color) Wake potential seen by the simulated bunch is shown by the red curve, which differs slightly from the wake potential of an ideal smooth Gaussian bunch shown in blue dashes. The difference shown by the magenta solid curve represents the random fluctuation of the finite number of macro-particles.

B. MICROWAVE INSTABILITY

Besides the accumulated growth from the uncompensated wake potential that we discussed above, there is still the issue of microwave instability. Even if the compensating rf systems can compensate for 100% of the wake potential of the realistic bunch, this only solves the problem of potential distortion, but not microwave instability. This is because the bunch linear distribution can be decomposed into $\rho = \rho_0 + \rho_1$, where ρ_0 is the time-independent *unperturbed* distribution which goes into Eq. (4.2) to be compensated by the rf systems. On the other hand, the *perturbed* distribution ρ_1 is time-dependent. It represents an infinitesimal deviation from the bunch distribution ρ_0. When it is substituted into Eq. (4.2), it can excite a voltage containing the collective modes of instability oscillating at some eigenfrequencies, thus enhancing the growth of those frequency components, unless the system is stable against perturbation. In other words, the accumulated growth due to potential-well distortion is a static solution while microwave instability is a time-dependent solution. Although the compensating rf systems cannot lower the growth rate of microwave instability, they do, however, reduce the total amount of growth by reducing the amount of ripples inside the bunch, which provide the seeds of the growth.

The Boussard-modified Keil-Schnell criterion can be rewritten in the form

$$n_r\omega_0\sqrt{\frac{|\eta|I_{\rm pk}|Z_\parallel/n|}{2\pi eE}} \le n_r\omega_0|\eta|\sigma_\delta \ , \tag{4.6}$$

$\omega_0/(2\pi)$ being the revolution frequency and $n_r = \omega_r/\omega_0$ the resonant harmonic. The left side is the raw microwave growth rate without damping and the right side the Landau damping rate. Substituting into Eq. (4.6), we find that the Landau damping rates on the right side are much smaller than the left side for the two bunches. Thus, the left side is a good representation of the actual e-folding growth rate, which amounts to, for the 4-cm and 13-cm bunches, respectively, $\sim 2.76\times10^3$ and $\sim 1.53\times10^3$ s^{-1}, or or $\sim 0.32\%$ and $\sim 0.18\%$ per turn.

Note that the accumulated growth from the uncompensated fluctuation of jitters, etc, is quite different from the growth due to microwave instability. For the former, the growth in energy fluctuations every turn will be exactly by the *same* amount as given by the energy jitters in Fig. 3 or 6 (if muon decay is neglected). This is because the wake potential of particles along the bunch does not depend on the energy distribution of the bunch, but only on its linear density and the latter is essentially unchanged since the particles do not drift much during the first 1000 turns. On the other hand, the initial growth due to microwave instability at a particular turn is proportional to the actual energy fluctuation at that turn and the evolution of the growth is exponential. Thus, although the growth due to microwave instability is small at the beginning, it will be much faster later on when the accumulated energy fluctuations become larger.

It is important to point out that the above mentioned growth rates are for only the resonant-frequency component of the bunch because Eq. (4.6) is in the frequency domain. Since there are many lower-frequency components in the bunch other than the resonant frequency; the growth rates for them are proportional to their frequencies and are therefore considerably smaller. As a result, the actual growth rates of the energy spread or bunch area due to microwave instability will be smaller than the estimation reported above.

We ran simulations by turning off the phase-slip factor to zero and see negligible difference from the lower plots of Figs. 2 and 5, showing that longitudinal microwave instability plays nearly no role here. However, when the simulations were performed for a few times the e-folding lifetime of the muons, we did see some small amount of extra growth in momentum spread that can only be attributed to microwave instability. As was stated before, the simulations depend very sensitively on the initial imperfection of the bunch. For example, when 1×10^6 macro-particles are used instead, the amount of growth due to microwave instability becomes more obvious, as a result of the larger statistical particle-number fluctuation. In

any case, we believe that the amount of growth due to microwave instability will always be less important than the accumulated growth due to uncompensated bunch imperfection. This is mainly due to the compensated rf's, the finite lifetime of the muons, and the choice of the small $|\eta|$.

Although the growths due to either energy-fluctuation accumulation or microwave instability can appear rather violent as is shown in, for example, Fig. 5, the local momentum spread along the bunch remains unchanged. This arrives from the fact that the beam is very close to the transition energy. There is negligible phase drift and therefore no phase-space dilution due to filamentation will occur. As a result, the amount of Landau damping given by the right-hand side of Eq. (4.6) will not be increased even when the growth has developed for a long time.

Microwave instability for a bunch beam close to the transition energy is an extremely important and interesting issue, and deserves much more investigation. Further results and comments will be devoted to a future publication.

It is important to point out that the lower plots of Figs. 2 and 5 *do not* indicate the actual particle distributions of the future muon bunches after 1000 turns. The actual growth depends on the initial linear bunch shape, and the deviation of the coupling impedance from being broadband. If the initial bunch shape is extremely smooth and the coupling impedance is close to a broadband, the total growth in 1000 turns may be very minimal. On the other hand, if the initial bunch distribution and the coupling impedance as a function of frequency are very rugged, it will provide a large seed and the final distribution after 1000 turn can be much more violent than those depicted in Figs. 2 and 5. Therefore, to prevent excessive growth in the energy spread, methods must be devised to smooth the bunch distribution after ionization cooling and linac acceleration. To accomplish this, one needs to understand the source of noise fluctuation in a particle bunch. A measurement of the Tevatron bunch at Fermilab shows in Fig. 7 a spectral tail which is flat and extend up to a few GHz without any sign of rolling off, although the spectrum for the ideal smooth Tevatron bunch should roll off rapidly around 1 or 2 GHz [10]. Such fluctuations have also been considered as the source of the ear-growing bunch profile observed, where the jitters around the synchronous phase give rise to small beamlets which rotate around the main bunch with possibly multiples of the synchrotron frequency [11]. Although thermal noise has been suggested as a source of the fluctuation, the full understanding is still unknown. During the commissioning of the Fermilab Main Injector, the bunches exhibit very nonsmooth profiles soon after their injection. Some typical profiles are shown in Fig. 8. In the muon collider ring, the muon bunches inherit all their bunch imperfection from the processes of pion decay, muon cooling,

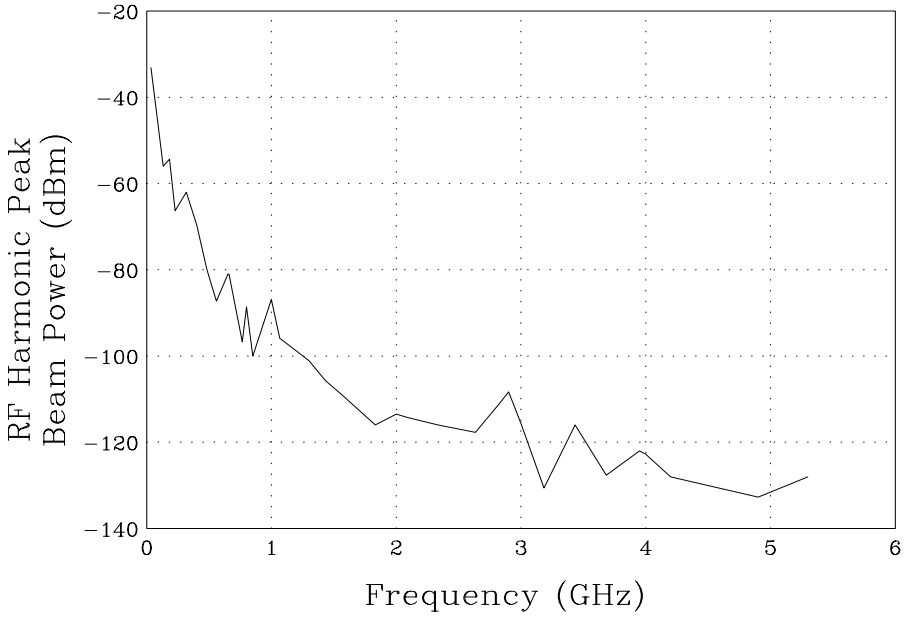

Figure 7: Beam current power spectrum of the Tevatron, measured at each harmonic of the RF frequency.

rf rotations, and muon acceleration. One expects the noises and imperfections of the muon bunches can be worse than the Tevatron bunches if no special action is taken.

Further reduction in impedance will lower the accumulated growth of the energy jitters. Since the growth increases with frequency also, one must try to smooth the vacuum chamber so that the impedance contribution at high frequencies and sharp resonances will be reduced to a minimum. On the other hand, reduction in the phase-slip factor will not help much because we believe that microwave instability would play only a secondary role here when $|\eta| \lesssim 1 \times 10^{-6}$.

C. RF CAVITIES AND BEAMLOADING

For a cavity of gap length ℓ and resonant frequency $\omega/(2\pi)$, the rf voltage at time t is

$$V(t) = V_0 \sin(\omega t + \varphi) \ , \tag{4.7}$$

where V_0 is the peak rf voltage. Suppose the center of the bunch passes through the center of the cavity gap at time $t = 0$. A beam particle at distance z at $t = 0$ behind the the bunch center travels according to $z' = -z + ct$. Thus, the integrated voltage sampled by this

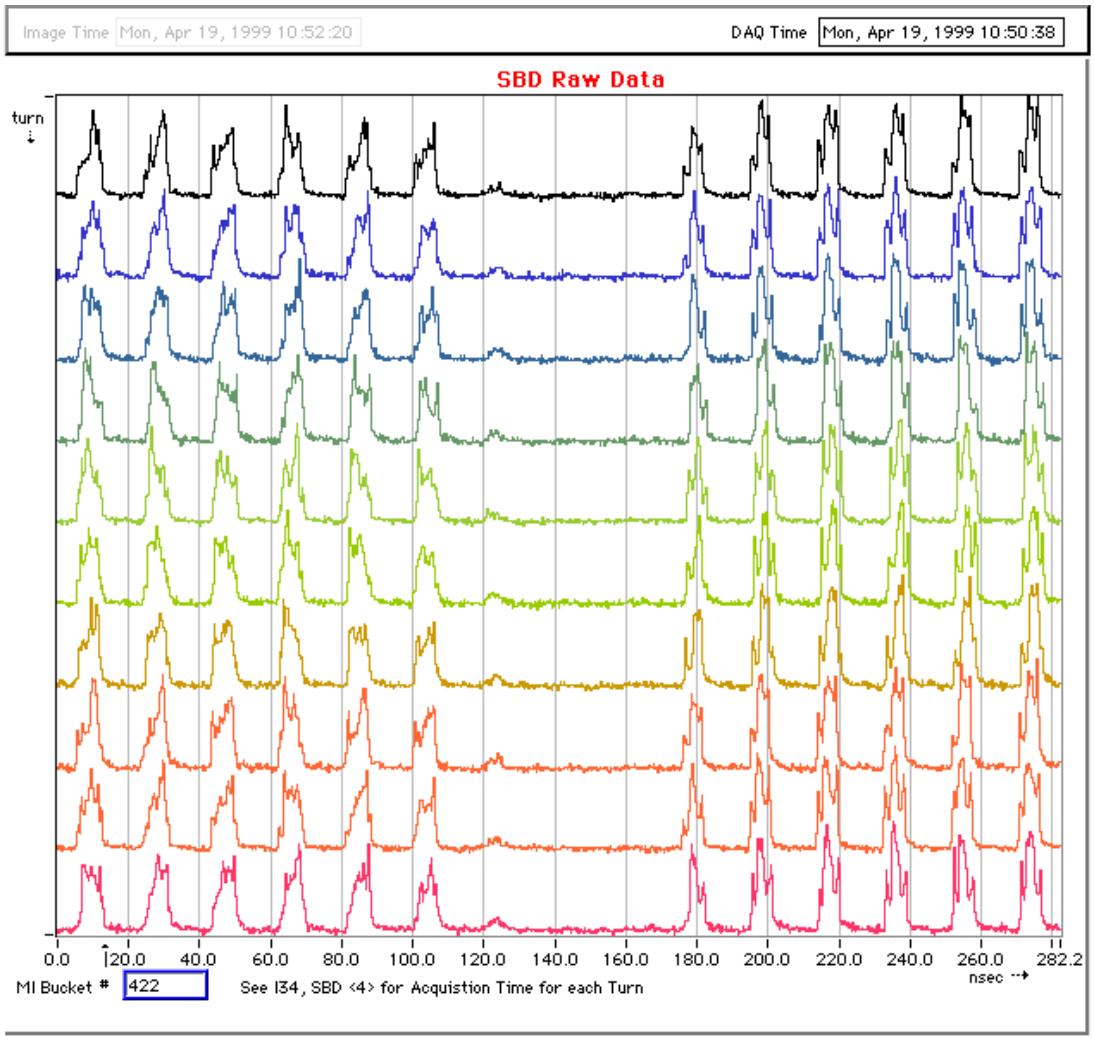

Figure 8: (color) Main Injector bunches $\sim$ 30 ms after the injection of the 6th batch at 8-turn booster injection, corresponding to an intensity of about 2.4×10^{10} protons per bunch. Consecutive traces are 12 turns ($\sim$ 130 μs) apart. Bunches directly from the booster seem to be clean and well behaved.

particle across the gap of the cavity is

$$\int_{-\ell/2}^{\ell/2} V(t)dz' = \int_{-\ell/2}^{\ell/2} dz' V_0 \sin\left(\frac{\omega z'}{c} + \varphi + \frac{\omega z}{c}\right) = V_0 \ell \sin\left(\frac{\omega z}{c} + \varphi\right) \left\{\frac{\sin[\omega\ell/(2c)]}{\omega\ell/(2c)}\right\} \ . \quad (4.8)$$

The actual voltage seen by the particle has been diminished by the transit factor in the curly-bracketed term. Care must be exercised in choosing the length of the cavity so that the transit factor will not be too small. Take the 4-cm bunch as an example, a cavity length of $\ell = 7.5$ cm leads to transit factors of 0.8373 and 0.3731 for the resonant frequencies 1.290 and 2.673 GHz. Then, the actual peak voltages in the two cavities have to be increased to 0.8568 and 0.6793 MV, respectively, for the two frequencies, and the electric fields at the gaps become 11.42 and 9.057 MV/m. Such accelerating gradients are only 0.36 and 0.20 times the Kilpatrick limits [12], and should therefore be achievable in room-temperature cavities.

For the 13-cm bunch, because the compensating sinusoids are of frequencies 0.3812 and 0.7966 GHz, much lower than those for the 4-cm bunch, the transit factors for cavities having the same length of $\ell = 7.5$ cm are 0.9851 and 0.9359, respectively. The actual peak voltages in the two cavities will be 66.39 and 26.43 kV, and the electric fields 0.885 and 0.362 MV/m. The latter are only 0.046 and 0.014 times the Kilpatrick limits for the two frequencies.

Since the fundamental modes of the cavities are used for wake-potential compensations, the muon beams also excite these modes of oscillation when passing through the cavities. This is called transient beamloading. If the beamloading voltages are high, the muon bunches will be very much affected. The shunt impedance R_s divided by the quality factor Q is a geometric factor of the cavity independent of the wall resistivity of the cavity. When wall resistivity is small, perturbation calculation for the pill-box cavity gives for the TM_{0n0} mode,

$$\frac{R_s}{Q} = \frac{8Z_0}{x_{0n}^2 J_0'^2(x_{0n})} \frac{\sin^2[\omega_{0n0}\ell/(2c)]}{\omega_{0n0}\ell/(2c)} \ , \quad (4.9)$$

where x_{0n0} is the n-th zero of the Bessel function J_0, $\omega_{0n0} = x_{0n0}c/R$ the resonant angular frequency of the mode, and R the radius of the cavity. The beamloading voltage seen by a particle at a distance z behind the bunch center is exactly the same as Eq. (4.3), or

$$V(z) = -\frac{eN\omega_r R_s}{2Q\cos\phi_0} \mathcal{R}e\ e^{j\phi_0 - z^2/(2\sigma_\ell^2)} w\left[\frac{\sigma_\ell \omega_r e^{j\phi_0}}{c\sqrt{2}} - \frac{jz}{\sqrt{2}\sigma_\ell}\right] , \quad (4.10)$$

where now $\omega_r = \omega_{010}$ and $\sin\phi_0 = 1/(2Q)$ with Q being the quality factor of this cavity. For the fundamental or TM_{010} mode, $x_{010} = 2.4045$. Note that $eN\omega_{010}R_s/Q$ is a measure of the beamloading voltage if the bunch is of zero length and the quality factor of the resonant impedance is very high. This can also be seen from Eq. (4.10). When $\sigma_\ell \to 0$, the argument

Table II: Beamloading voltages for the 4 compensating cavities.

	Resonant Frequency (GHz)	$eN\omega_{010}R_s/Q$ (MV)	Beamloading Max (MV)	Beamloading Min (MV)
4-cm bunch	1.290	2.270	1.249	−0.647
4-cm bunch	2.673	2.097	0.222	−0.134
total			1.140	−0.699
13-cm bunch	0.381	0.274	0.158	−0.083
13-cm bunch	0.797	1.082	0.143	−0.096
total			0.155	−0.145

of the complex error function becomes imaginary and the complex error function behaves as

$$\lim_{\sigma_\ell \to 0} w\left(\frac{-jz}{\sqrt{2}\sigma_\ell}\right) = \lim_{\sigma_\ell \to 0} \frac{2}{\sqrt{\pi}}\, e^{z^2/(2\sigma_\ell^2)} \int_{-\frac{z}{\sqrt{2}\sigma_\ell}}^{\infty} e^{-t^2} dt = \begin{cases} 0 & z < 0\ , \\ 1 & z = 0\ , \\ 2 & z > 0\ , \end{cases} \tag{4.11}$$

and the transient beamloading voltage becomes

$$V(z) = \begin{cases} 0 & z < 0 \text{ (head)}\ , \\ -\dfrac{eN\omega_r R_s}{2Q\cos\phi_0} & z = 0 \text{ (center)}\ , \\ -\dfrac{eN\omega_r R_s}{Q\cos\phi_0} & z > 0 \text{ (tail)}\ . \end{cases} \tag{4.12}$$

With finite bunch lengths, the beamloading voltages will be smaller. We assume that during the operation mode of the 4-cm bunch, the gaps of the compensating cavities for the 13-cm bunch will be shorted and vice versa. Assuming the quality factor to be $Q = 100$, the beamloading voltages for the 4-cm bunch operation and 13-cm bunch operation are shown, respectively, in Figs. 9 and 10. Table II shows $eN\omega_{010}R_s/Q$ and the maxima and minima of the beamloading voltages of the four cavities. We assume that all higher-order modes of the cavities can be eliminated by designing absorbers or dampers. The beamloading voltages will be smaller if the quality factors of the cavities are smaller. However, a quality factor of $Q = 100$ is already very low for a non-ferrite-loaded cavity.

Note that these beamloading voltages are comparable to the wake potential voltages. In other words, the compensating cavities introduce new wake potentials comparable to those which they are supposed to compensate. These beamloading voltages must be removed. If

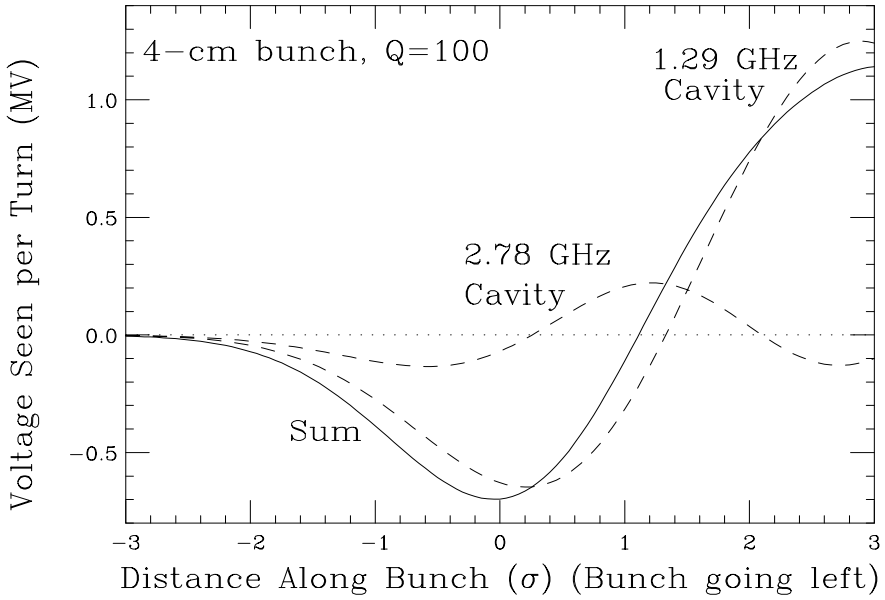

Figure 9: Beamloading voltages seen by particles in the 4-cm bunch as they traverse the wake-potential compensating cavities. The particles are at distance behind the bunch center in unit of rms bunch length.

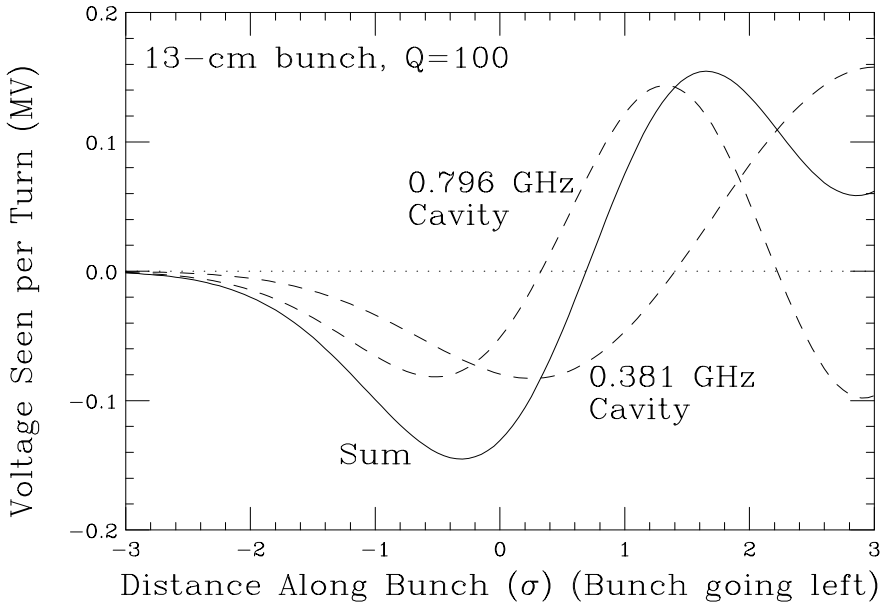

Figure 10: Beamloading voltages seen by particles in the 13-cm bunch as they traverse the wake-potential compensating cavities. The particles are at distance behind the bunch center in unit of rms bunch length.

not, the compensating cavities will have not been doing their jobs properly. One suggestion is to optimize the parameters, such as frequencies, voltages, and phases, of these cavities, so that they will cancel not only the wake potential due to the longitudinal coupling impedance of the vacuum chamber, but also the wake potential or transient beamloading of the compensating cavities themselves as well. This, however, appears to be impossible, because the beam loading voltages are of different frequencies from the compensating rf voltages.

Another suggestion is to use a feed-forward system. First, let us understand how the transient beamloading occurs. As the bunch of say μ^+ passes through the cavity gap, a negative charge equal to that carried by the bunch will be left by the image current at the upstream end of the cavity gap. Since the negative image current will resume from the downstream end of the cavity gap following the bunch, an equal amount of positive charge will accumulate there. Thus, a voltage will be created at the gap opposing the beam current and this is the transient beamloading voltage as illustrated in Fig. 11. For an infinitesimally short bunch, this transient voltage is

$$V_t \sim \frac{eN}{C} = \frac{eN\omega_r R_s}{Q} \ , \tag{4.13}$$

where C is the equivalent capacitance across the gap of the cavity. For a bunch of finite length, the transient beamloading voltages seen by different parts of the beam will become what is shown in Figs. 9 and 10. The Fermilab future low-energy booster which is destined to be used as the proton driver for the muon collider project has rather strong transient beamloading voltage. Griffin [13] suggested to use a feed-forward system, which will monitor the linear charge distribution of the bunch and deliver via a tetrode the same amount of negative charge density to the downstream end of the cavity gap so as to cancel the positive charge there and thus alleviating the transient beamloading. This feed-forward solution for the proton driver is illustrated in Fig. 12. Some similar scheme should also work to solve the beamloading issues for the compensating cavities in the muon colliding ring.

V. TRANSVERSE MICROWAVE INSTABILITY

The Keil-Schnell-like stability criterion for transverse microwave instability can be written as [14]

$$\frac{eI_{\rm pk}|Z_\perp|c}{4\pi E\nu_\beta} \le \frac{4\sqrt{2}\omega_0}{\pi}|(n_r-\nu_\beta)\eta+\xi|\sigma_\delta \ , \tag{5.1}$$

where the left side is the raw growth rate without damping and the right side the damping rate. In above, ξ is the chromaticity, $\nu_\beta \approx 6.24$ is the betatron tune, and only the tune

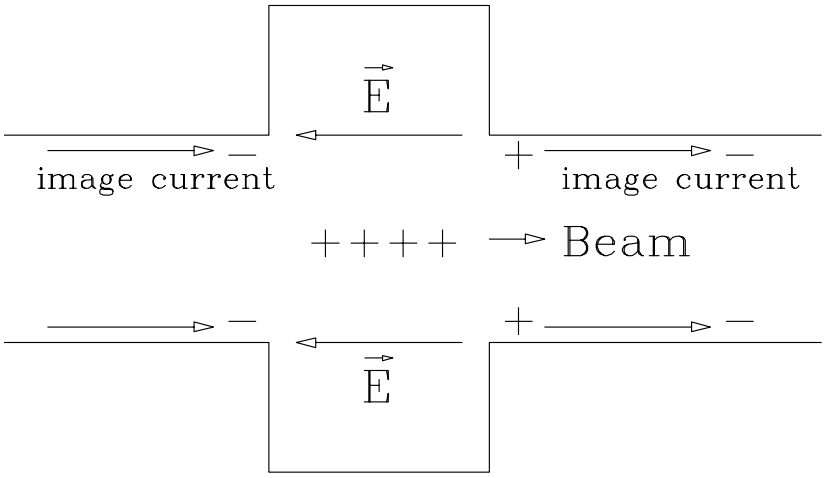

Figure 11: As a positively charged bunch passes through a cavity, the image current leaves a negative charge at the upstream end of the cavity gap. As the image current resumes at the downstream side of the cavity, a positive charge is created at the downstream end of the gap because of charge conservation, thus setting up an electric field $\vec{E}$ and therefore the transient beamloading voltage.

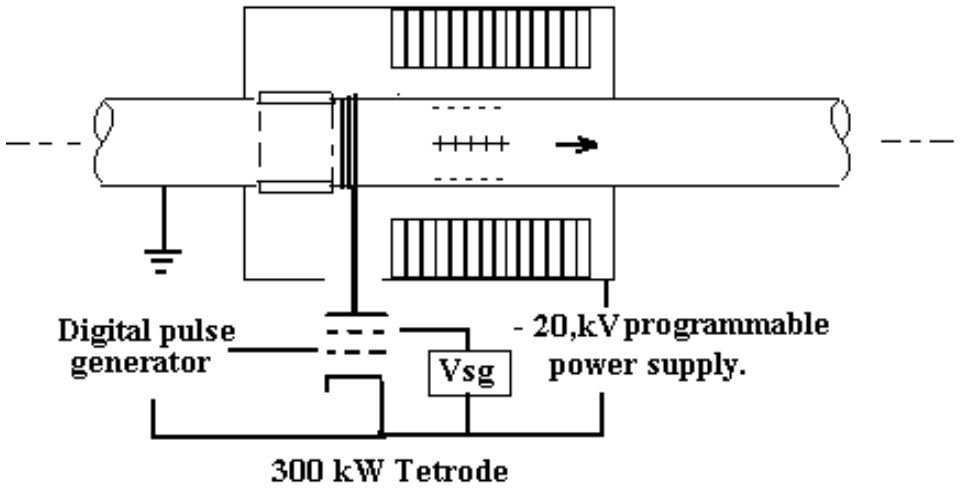

Figure 12: In the design of the future Fermilab proton driver, the beam linear charge density is monitored and fed into a tetrode, which supplies the same charge density to the downstream end of the cavity gap. Thus the transient beamloading voltage is cancelled.

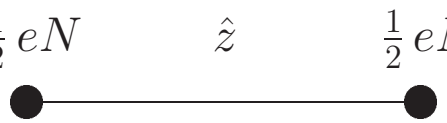

Figure 13: The two-particle model, where the bunch is represented by two macro-particles each carrying half the charge of the bunch separated by a distance $\hat{z}$.

spread resulting from momentum spread has been included. Here, we assume a broadband impedance with $Q = 1$, $Z_\perp = 0.1$ MΩ/m at the angular resonant frequency of $\omega_r = 50$ GHz. The raw growth rates are 14.7×10^3 and 4.51×10^3 s^{-1}, respectively, for the 4-cm bunch and 13-cm bunch. For stabilization, one requires $|(n_r - \nu_\beta)\eta + \xi| > 1.3$ and 16, respectively, for the two bunches. The phase-slip factor $|\eta| = 1 \times 10^{-6}$, however, is too small to contribute any damping at all. But stability can still be maintained if the chromaticities are larger than 1.3 and 16. Octupoles can also be installed to provide additional amplitude-dependent tune spread. In that case the amount of chromaticity for stabilization can be reduced. Since we are interested in only 1000 turns, one may be able to tolerate a small growth if it is not too serious.

VI. TRANSVERSE BEAM BREAKUP

Since bunch particles do not move much longitudinally with respect to the bunch center during their lifetime, any off-axis particle will affect its followers constantly leading to beam breakup in exactly the same way as a bunch traveling along a linac.

A. TWO-PARTICLE MODEL

Take the simple two-particle model in Fig. 13, by which the bunch is represented by two macro-particles of charge $\frac{1}{2}eN$ separated by a distance $\hat{z}$. The transverse displacements of the head, y_1, and the tail, y_2, satisfy

$$\frac{d^2y_1}{ds^2} + \frac{\nu_{\beta_1}^2}{R^2}\,y_1 = 0\ , \tag{6.1}$$

$$\frac{d^2y_2}{ds^2} + \frac{\nu_{\beta_2}^2}{R^2}\,y_2 = -\frac{e^2NW_1(\sigma_\ell)}{2CE}\,y_1\ , \tag{6.2}$$

where s is the longitudinal distance measured along the on-momentum closed orbit, and $C = 2\pi R$ is the circumference of the collider ring. This model has been giving a reasonably

accurate description to the beam breakup mechanism for short electron bunches when $\hat{z}$ is taken as twice the rms bunch length. The head oscillates as $y_1(s) = y_{10}\cos(\nu_{\beta_1} s/R)$ and the tail is initially at $y_2 = y_{10}$ with $y_2' = 0$. The displacement of the tail can be readily solved and the result is

$$y_2(s) = y_{10}\cos\frac{\bar{\nu}_\beta s}{R}\cos\frac{\Delta\nu_\beta s}{2R} - \left[\frac{e^2 N W_1(\hat{z})R}{4\pi E\bar{\nu}_\beta} + \Delta\nu_\beta\right]\left[y_{10}\sin\frac{\bar{\nu}_\beta s}{R}\right]\left[\frac{\sin\Delta\nu_\beta s/(2R)}{\Delta\nu_\beta}\right] \ , \quad (6.3)$$

where $\bar{\nu}_\beta = \frac{1}{2}(\nu_{\beta_1} + \nu_{\beta_2})$ is the mean of the two betatron tunes of the head and tail. When the tune difference $\Delta\nu_\beta = \nu_{\beta_2} - \nu_{\beta_1}$ approaches zero, the tail is driven resonantly by the head and its displacement grows linearly with s:

$$y_2(s) = y_1(s) - \frac{e^2 N W_1(\hat{z})}{8\pi E\nu_\beta}\left[y_{10}\sin\frac{\nu_{\beta_1} s}{R}\right] s \ . \quad (6.4)$$

In a length L, the displacement of the tail will grow by Υ folds, where [15]

$$\Upsilon = -\frac{e^2 N W_1(\hat{z})\langle\beta\rangle L}{8\pi E R} \ . \quad (6.5)$$

In the above, we have written $\nu_\beta = R/\langle\beta\rangle$. This is because the transverse impedance initiates a kick y' of the beam and the size of the kicked displacement depends on the betatron function at the location of the impedance. This can be easily visualized from the transfer matrix.

For a broadband impedance, the transverse wake function at a distance z behind the source particle is, for $z > 0$,

$$W_1(z) = -\frac{\omega_r^2 Z_\perp}{Q\bar{\omega}}\, e^{-\alpha z/c}\sin\frac{\bar{\omega} z}{c} \ , \quad (6.6)$$

where $Z_\perp$ is the transverse impedance at the angular resonant frequency ω_r, which is shifted to $\bar{\omega} = \sqrt{\omega_r^2 - \alpha^2}$ by the decay rate $\alpha = \omega_r/(2Q)$ of the wake. Let us introduce the dimensionless variables

$$v = \frac{\omega_r\sigma_\ell}{c} \ , \quad t = \frac{z}{\sigma_\ell} \ , \quad \text{and} \quad \phi = vt\cos\phi_0 = \frac{\bar{\omega} z}{c} \ , \quad (6.7)$$

where the angle ϕ_0 is defined as

$$\cos\phi_0 = \sqrt{1 - \frac{1}{4Q^2}} \quad \text{or} \quad \sin\phi_0 = \frac{1}{2Q} \ , \quad (6.8)$$

assuming that $Q > \frac{1}{2}$. Then, the transverse wake in Eq. (6.6) can be rewritten as, for $\phi > 0$,

$$W_1(\phi) = -2\omega_r Z_\perp \tan\phi_0 \sin\phi\, e^{-\phi\tan\phi_0} \ , \quad (6.9)$$

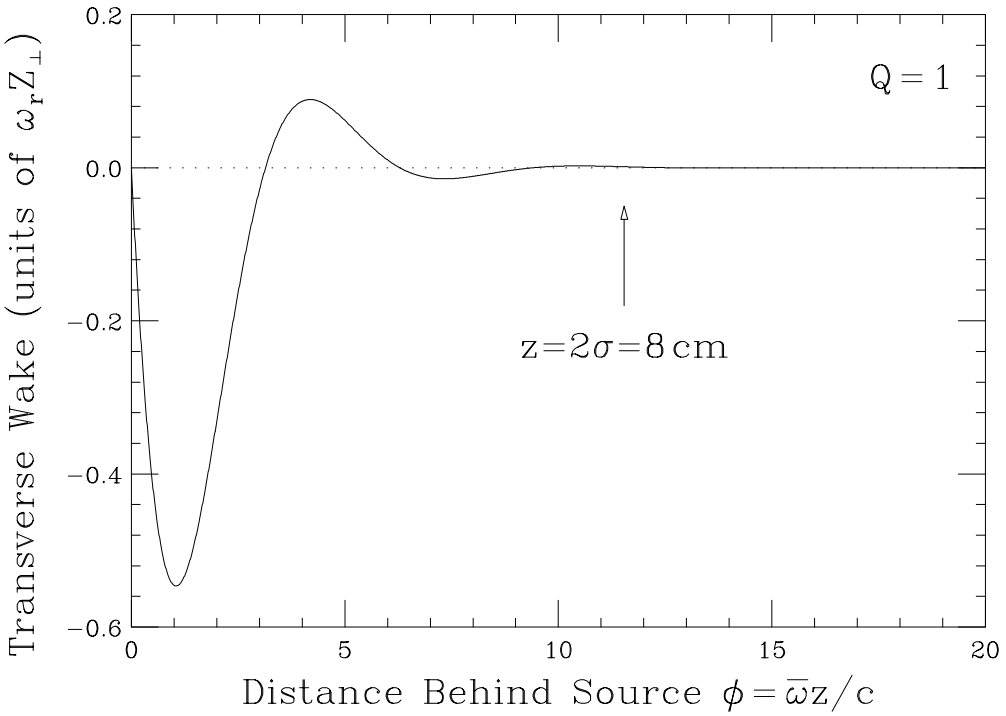

Figure 14: Transverse wake function for a broadband impedance with $Q = 1$ in units of $\omega_r Z_\perp$ as a function of $\phi = \bar{\omega} z/c$ behind the source. With resonant angular frequency $\omega_r = 50$ GHz, the position for $z = 2\sigma_\ell$ for the 4-cm bunch is marked, and that for the 13-cm bunch is at $\phi = 37.5$. The plot shows that some part of the bunch other than the tail will be affected most.

The wake function decreases linearly from zero when $\phi = \bar{\omega} z/c \ll 1$ and reaches a minimum

$$W_1|_{\min} = -2\omega_r Z_\perp \tan\phi_0 \cos\phi_0 \, e^{-\left(\frac{\pi}{2}-\phi_0\right)\tan\phi_0} \tag{6.10}$$

at

$$\phi = \frac{\pi}{2} - \phi_0 \quad \text{or} \quad \frac{\alpha z}{c} = \left(\frac{\pi}{2} - \phi_0\right) \tan\phi_0 \ . \tag{6.11}$$

After that it oscillates with amplitude decaying at the rate of $\alpha = \omega_r/(2Q)$, crossing zero at steps of $\Delta\phi = \bar{\omega} z/c = \pi$. This is illustrated in Fig. 14. Notice that the position of the minimum $z_{\min} = c\left(\frac{\pi}{2} - \phi_0\right)/(\omega_r \cos\phi_0)$ is much less than the rms bunch length, showing that some part of the bunch other than the tail will be affected most.

In other words, the two-particle model is not so applicable in our situation where the bunch is long and the resonant frequency is high. The two-particle model works well only when the tail macro-particle lies within the linear part of the transverse wake, when ϕ or

$v \ll 1$. Nevertheless, as an estimate, we can substitute W_1 in Eq. (6.5) by its minimum value and take $\nu_\beta = 6.24$. We find that the displacements of some particles along the bunch will be doubled in ~ 21 turns for the 4-cm bunch, which is possibly an overestimate.

For a bunch with linear density $\rho(z)$, the transverse motion $y(z,s)$ at a distance z behind the bunch center and 'time' s is given by

$$\frac{d^2y(z,s)}{ds^2} + \frac{\nu_\beta^2}{R^2}\, y(z,s) = -\frac{e^2N}{CE}\int_{-\infty}^{z} dz'\rho(z')W_1(z-z')y(z',s)\ . \tag{6.12}$$

This equation can be solved first by letting $y(z,s)$ be a free oscillation on the right-hand side and solving for the displacement $y(z,s)$ on the left-hand side. Then, iterations are made until the solution becomes stable. Therefore, when Υ is large, the growth will be proportional to powers of Υ and even exponential in Υ. Thus, $\langle\beta\rangle Z_\perp$, ω_r, as well as Q can be very sensitive to the growth.

Simulations have been performed for the 4-cm and 13-cm bunches with a betatron tune $\nu_\beta \sim 6.24$, interacting with a broadband impedance with $Q = 1$ and $Z_\perp = 0.1$ MΩ/m at the angular resonant frequency $\omega_r = 50$ GHz. Initially, a bunch is populated with a vertical Gaussian spread of $\sigma_y = 3$ mm and $y' = 0$ for all particles. There is no offset for the center of the bunch. Ten thousand macro-particles are used to represent the bunch intensity of 4×10^{12}. The half-triangular bin size is 15 ps (or 0.45 cm). In Figs. 15 and 16, we show the total growth of the *normalized* beam size $\sigma_y \equiv \langle y^2 + (\langle\beta\rangle y')^2\rangle^{1/2}$ relative to the initial beam size up to 1000 turns for various values of $\langle\beta\rangle$, respectively, for the 13-cm and 4-cm bunches. The turn-by-turn decay of the muons has been taken into account. We see that the beam size grows very much faster for larger betatron function. Also the growths for the 4-cm bunch are much larger than those for the 13-cm bunch because the linear charge density of the former is larger.

B. TUNE SPREAD

Kim, Wurtele, and Sessler [16] suggested to suppress the growth of the transverse beam breakup by a small tune spread in the beam, coming either through chromaticity, amplitude dependency, or beam-beam interaction. This is because a beam particle will be resonantly driven by only a small number of particles in front that have the same betatron tune.

To implement this, we add a detuning term

$$\Delta\nu_{\beta_i} = a[y_i^2 + (\langle\beta\rangle y_i')^2] \tag{6.13}$$

to the i-th particle, as if it is contributed by an octupole or sextupole. In Figs. 17 and 18, we plot the growths of the normalized beam size relative to the initial beam size with

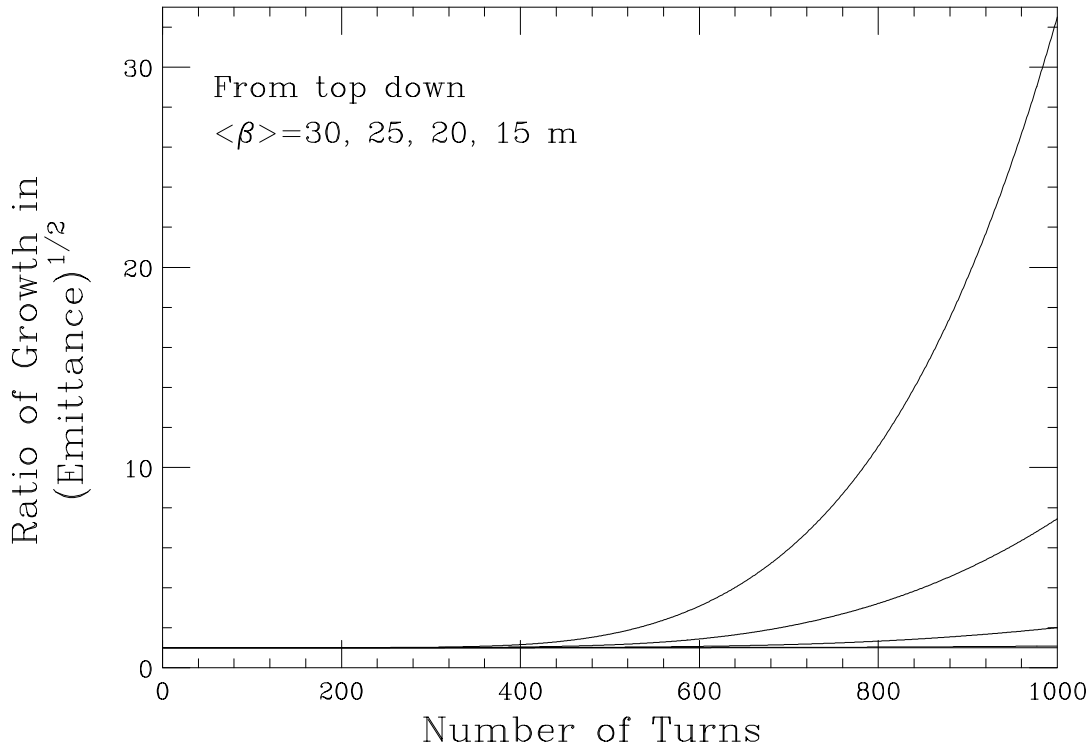

Figure 15: Beam-breakup growth of the 13-cm bunch interacting with a broadband impedance of $Q = 1$, $Z_\perp = 0.1$ MΩ/m at the angular resonant frequency of $\omega_r = 50$ GHz. The total growths at 1000 turns reach 32.50, 7.4, 2.0, 1.09, 1.006, respectively for $\langle\beta\rangle = 30$, 25, 20, 15, 10 m.

various rms tune spreads $\sigma_{\nu_\beta} = a\langle\sigma_y^2 + (\langle\beta\rangle\sigma_{y'})^2\rangle$. Here, an average betatron function of $\langle\beta\rangle = 20$ m has been used. This is because BPMs, which contribute significantly to the transverse impedance, are usually installed at locations where the betatron function is large. We see that to damp the growth of the 13-cm bunch to less than 1%, we need a rms tune spread of $\sigma_{\nu_\beta} = 0.0008$ or a total tune spread of $\Delta\nu_\beta = 3\sigma_{\nu_\beta} = 0.0024$. On the other hand, to damp the growth of the 4-cm bunch to less than 1%, we need a rms tune spread of $\sigma_{\nu_\beta} = 0.006$ or a total tune spread of $\Delta\nu_\beta = 3\sigma_{\nu_\beta} = 0.024$. However, if the transverse impedance is larger, the average betatron function is larger, the resonant frequency is larger, or the quality factor is smaller, this required tune spread may become too large to be acceptable. This is because a large amplitude-dependent tune spread can lead to reduction of the dynamical aperture of the collider ring.

For the lattice of the ring designed by Trbojevic and Ng [1], in order to allow for a larger

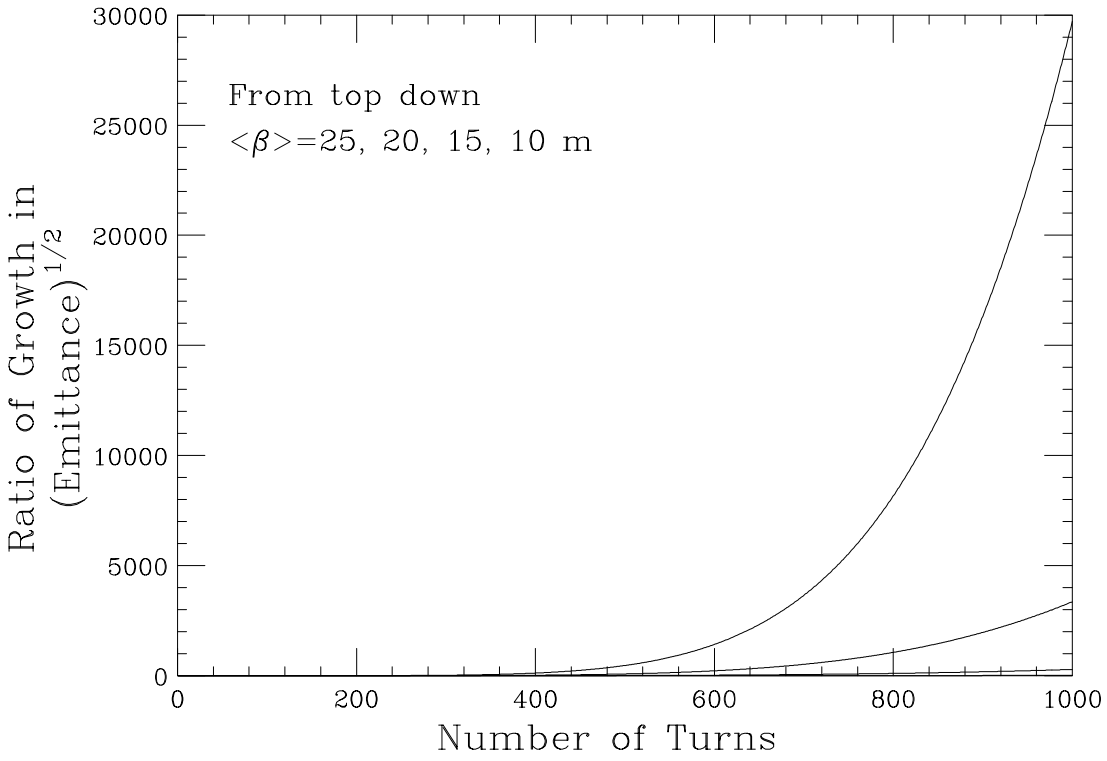

Figure 16: Beam-breakup growth of the 4-cm bunch interacting with a broadband impedance of $Q = 1$, $Z_\perp = 0.1$ MΩ/m at the angular resonant frequency of $\omega_r = 50$ GHz. The total growths at 1000 turns reach 29713, 3361, 287, 16.2, respectively for $\langle\beta\rangle = 25$, 20, 15, 10 m.

enough momentum aperture, the amplitude-dependent tune shifts are

$$\begin{aligned} \nu_{\beta x} &= 8.126 - 100\epsilon_x - 4140\epsilon_y \\ \nu_{\beta y} &= 6.240 - 4140\epsilon_x - 50.6\epsilon_y \end{aligned} \tag{6.14}$$

for the on-momentum particles, where the unnormalized emittances ϵ_x and ϵ_y are measured in πm. For the 4-cm bunch, the normalized rms emittance is $\epsilon_{\rm Nrms} = 85 \times 10^{-6}$ πm. Since the muon energy is 50 GeV, the unnormalized rms emittance is $\epsilon_{\rm rms} = 1.80 \times 10^{-7}$ πm, and becomes 1.62×10^{-6} πm when 3σ are taken. Thus, the allowable tune spread for the on-momentum particles is $\Delta\nu_\beta = 4140\,\epsilon_y = 0.0067$. Tune spreads larger than this will lead to much larger tune spreads for the off-momentum particles, thus reducing the momentum aperture of the collider ring. For 4-cm bunch, to damp beam breakup to about 1% when $Z_\perp = 0.1$ MΩ/m and $\langle\beta\rangle = 20$ m, one needs $\Delta\nu_\beta = 0.024$. However, we do not know exactly what $\langle\beta\rangle$ and $Z_\perp$ are. Simulations show that if $\langle\beta\rangle Z_\perp$ becomes doubled, 2.5 times, 5 times, and 10 times, the tune spreads required jump to, respectively, ~ 0.054, 0.073, 0.18, and 0.54.

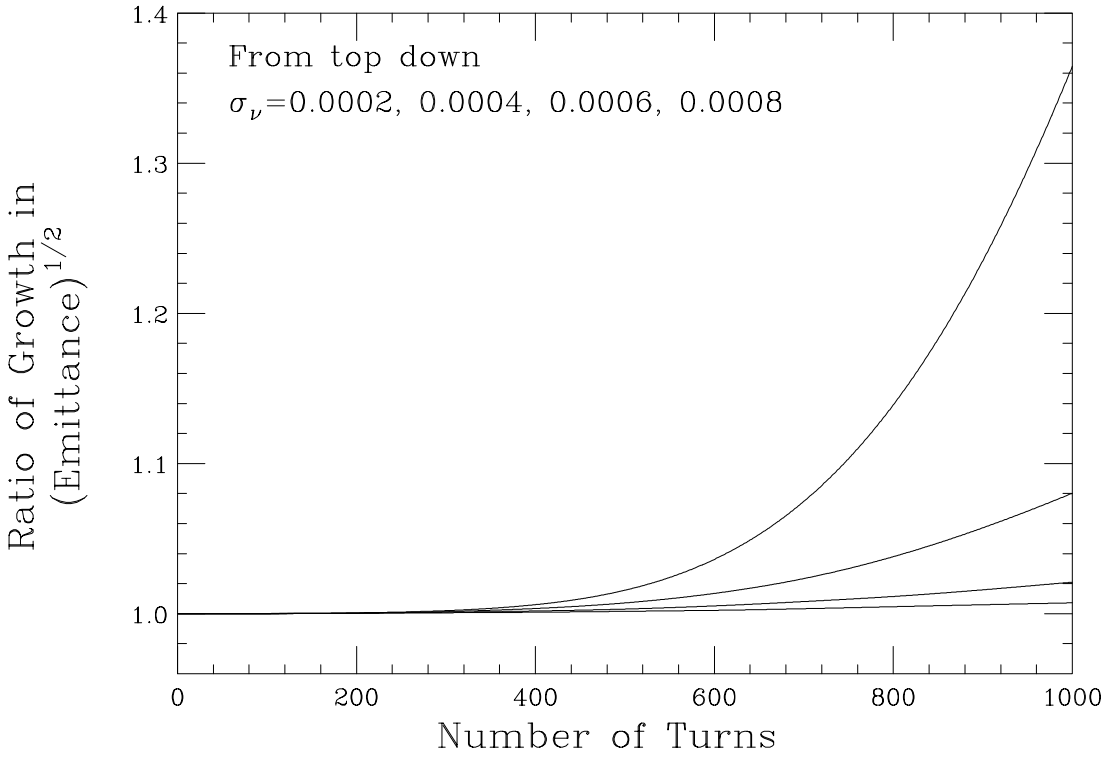

Figure 17: Total growth of the 13-cm bunch within the 1000 turns in the presence of an amplitude dependent tune shift, such as provided by an octupole. The maximum growths are 1.36, 1.08, 1.02, 1.007, respectively for rms tune spread of $\sigma_{\nu_\beta} = 0.0002$, 0.0004, 0.0006, 0.0008. An average betatron function of $\langle\beta\rangle = 20$ m has been assumed.

Thus, it appears that pure tune spread may be able to damp beam breakup for the 13-cm bunch but may not work for the 4-cm bunch. Although tune spreads due to chromaticity and beam-beam interaction will also damp beam breakup, it is unclear how much the momentum aperture will be reduced due to these tune spreads.

C. BALAKIN-NOVOKHATSKY-SMIRNOV DAMPING

The transverse beam breakup can be cured by varying the betatron tune of the beam particles along the bunch, so that resonant growth can be avoided. In the two-particle model, we can set

$$\Delta\nu_\beta = -\frac{e^2 N W_1(\hat{z}) R}{4\pi E \bar{\nu}_\beta} \ , \tag{6.15}$$

in Eq. (6.3), so that the tail will be oscillating in phase and with the same amplitude and

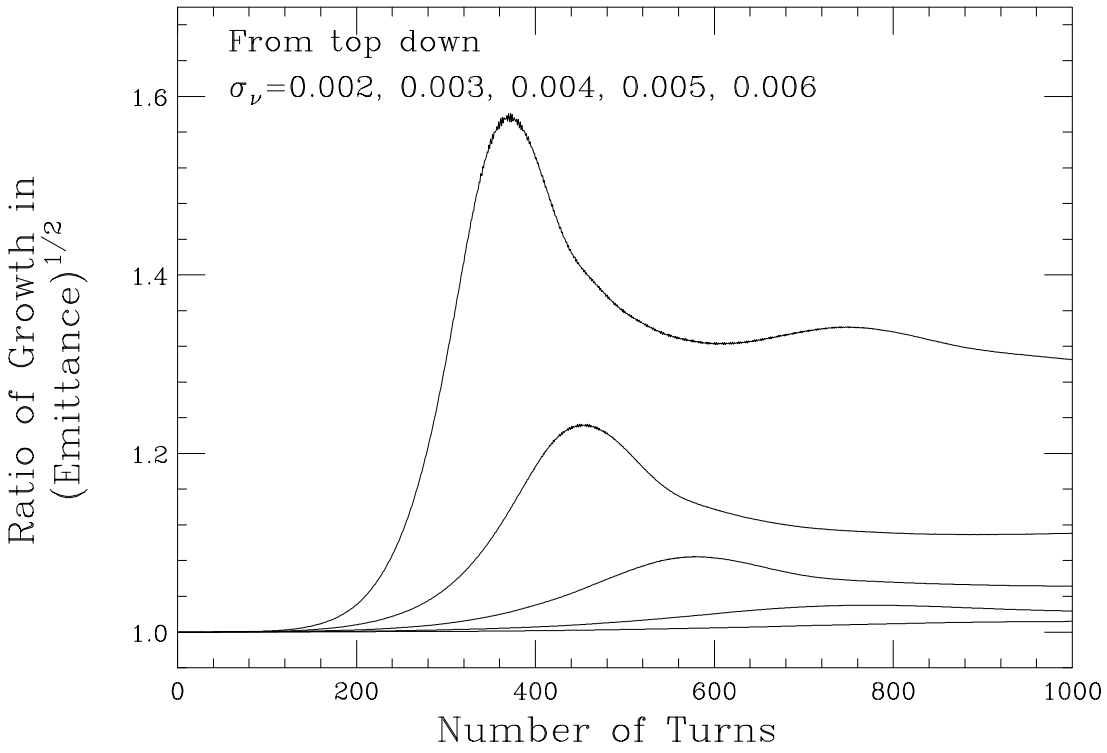

Figure 18: Total growth of the 4-cm bunch within the 1000 turns in the presence of an amplitude dependent tune shift, such as provided by an octupole. The maximum growths are 1.23, 1.58, 1.08, 1.03, 1.012, respectively for rms tune spread of $\sigma_{\nu_\beta} = 0.002$, 0.003, 0.004, 0.005, 0.006. An average betatron function of $\langle\beta\rangle =$ 20 m has been assumed.

tune as the head. The is known as Balakin-Novokhatsky-Smirnov (BNS) damping [17].

For a particle-distributed bunch, in order that all particles will perform betatron oscillation with the same frequency and same phase after the consideration of the perturbation of the transverse wake, special focusing force is required to compensate for the variation of unperturbed betatron tune along the bunch. With the linear distribution $\rho(z)$, the equations of motion of Eq. (6.2) in the two-particle model generalize to

$$\frac{d^2y(z,s)}{ds^2} + \frac{[\nu_\beta + \Delta\nu_\beta(z)]^2}{R^2}\, y(z,s) = -\frac{e^2N}{CE}\int_{-\infty}^{z} dz'\rho(z')W_1(z-z')y(z',s)\ , \tag{6.16}$$

where $z > 0$ denotes the tail and $z < 0$ the head, or the bunch is traveling towards the left. We need to choose the compensation $\Delta\nu_\beta(z)$ along the bunch in such a way that the betatron oscillation amplitude

$$y(z,s) \sim \sin\left(\frac{\nu_\beta}{R}\, s + \varphi_0\right) \tag{6.17}$$

is independent of z, the position along the bunch, with φ_0 being some phase, because only in this way any particle will not be driven by a resonant force from any particle in front. The solution is then simply

$$\frac{2\nu_\beta\Delta\nu_\beta + \Delta\nu_\beta^2(z)}{R^2} = -\frac{e^2N}{CE}\int_{-\infty}^{z} dz'\rho(z')W_1(z-z') \ , \tag{6.18}$$

or, for small compensation $\Delta\nu_\beta(z)$,

$$\frac{\Delta\nu_\beta(z)}{\nu_\beta} = -\frac{e^2NR}{4\pi\nu_\beta^2E}\int_{-\infty}^{z} dz'\rho(z')W_1(z-z') \ . \tag{6.19}$$

If the linear bunch distribution $\rho(z)$ is a Gaussian interacting with a broadband impedance, the integration can be performed exactly to give

$$\frac{\Delta\nu_\beta(z)}{\nu_\beta} = \frac{e^2NR}{4\pi\nu_\beta^2E}\frac{\omega_r^2Z_\perp}{2\bar{\omega}Q}e^{-z^2/(2\sigma_\ell^2)}\,\mathcal{I}m\,w\left[\frac{ve^{j\phi_0}}{\sqrt{2}} - \frac{jz}{\sqrt{2}\sigma_\ell}\right] \ , \tag{6.20}$$

where w is the complex error function while $\sin\phi_0 = 1/(2Q)$ and $v = \omega_r\sigma_\ell/c$ as defined in Eqs. (6.7) and (6.8). For long bunches and high resonant frequency, or $v \gg Q$, the complex error function behaves as

$$w(z) = \frac{j}{\sqrt{\pi}z} + \mathcal{O}\left(\frac{1}{|z|^3}\right) \ . \tag{6.21}$$

This is certainly satisfied by both the 4-cm and 13-cm bunches, where $v = 6.67$ and 21.7, respectively. Then, the relative tune-shift compensation in Eq. (6.20) can be simplified to

$$\frac{\Delta\nu_\beta(z)}{\nu_\beta} \approx \frac{e^2N\omega_rZ_\perp R}{2(2\pi)^{3/2}\nu_\beta^2QvE}\left[1 + \frac{z}{vQ\sigma_\ell}\right]e^{-z^2/(2\sigma_\ell^2)} \ . \tag{6.22}$$

The relative tune-shift compensations required for the two bunches are shown in Fig. 19. Note that in Eq. (6.22), vQ controls the asymmetry of the tune-shift compensation curve. When $vQ \to \infty$, there is no asymmetry and the compensation curve reduces to just a Gaussian, and, at the same time, $\Delta\nu_\beta/\nu_\beta$ decreases to zero. On the other hand, when $v \ll Q$ for short bunches and low broadband resonant frequency, the relative tune-shift becomes rather linear as depicted by the $v = 0.3$ curve in Fig. 20. The curve for the 4 cm bunch ($v = 6.67$) is also shown for comparison. This is the situation for BNS damping of short electron bunches, which is very different from the BNS damping for the muon bunches that we discuss here.

To cure beam breakup with BNS damping in an electron linac, the electron bunch is usually placed near the crest of the rf wave so that the head and tail of the bunch will acquire slightly different energies, and therefore slightly different betatron tunes through

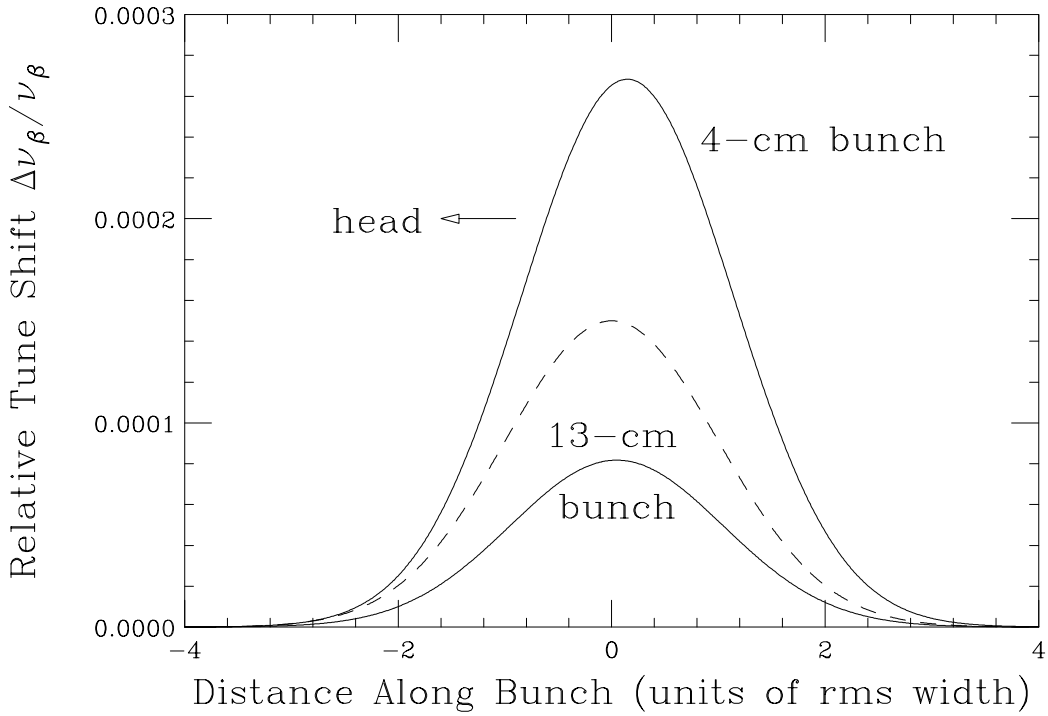

Figure 19: Relative tune shift compensation for beam particles at distance z/σ_ℓ behind the bunch center (or bunch going to the left) to cure beam breakup for the 4-cm and 13-cm bunches. The bunch profile is plotted in dashes as a reference.

chromaticity. For muon bunches in the collider ring, however, this method cannot be used. A rf quadrupole must be installed and pulsed according to the compensation curve for each bunch as the bunch is passing through it. The tune-shift compensation is fitted by a superposition of two sinusoids with frequencies $f_i = \omega_i/(2\pi)$,

$$\frac{\Delta\nu_\beta}{\nu_\beta} = \sum_{i=1}^{2} \left(\frac{\Delta\nu_\beta}{\nu_\beta}\right)_i \cos\left(\frac{\omega_i z}{c} + \varphi_i\right) \ . \tag{6.23}$$

The best fits for the two bunches are listed in Table III. If a rf quadrupole of length ℓ is built for the tune compensation, the magnetic flux gradient is

$$B'(t) = B'_0 \cos(\omega t + \varphi) \ , \tag{6.24}$$

where B'_0 is the maximum magnetic flux gradient. Suppose the center of the bunch passes through the quadrupole at time $t = 0$. A beam particle at distance z behind the bunch center when $t = 0$ travels according to $z' = -z + ct$. Thus, the integrated magnetic flux

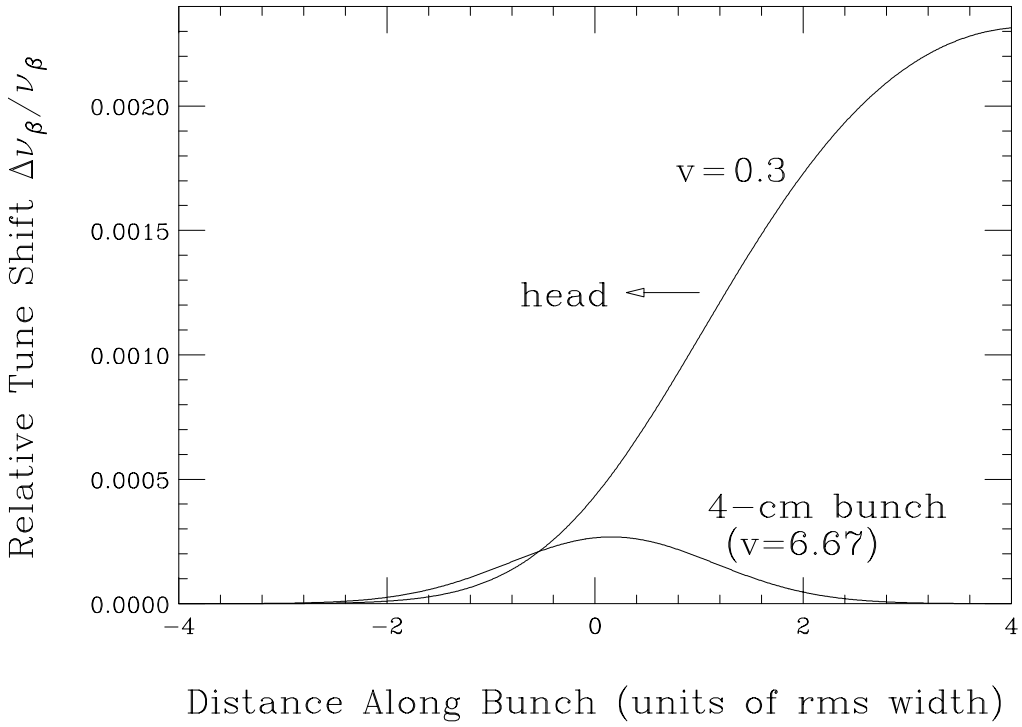

Figure 20: Relative tune shift compensation for beam particles at distance z/σ_ℓ behind the bunch center (or bunch going to the left) to cure beam breakup for a short bunch interacting with a broadband impedance at lower frequency, $v = \omega_r\sigma_\ell/c = 0.3$. The curve for the 4-cm bunch, where $v = 6.67$, is plotted as comparison. Note that when v is small, the compensation is more linear, or is of much lower frequency.

Table III: Two-sinusoidal fits for tune-shift compensation.

	$(\Delta\nu_\beta/\nu_\beta)_i$	harmonic	f_i (GHz)	φ_i (rad)
4-cm bunch	2.074×10^{-4}	794	0.680	0.0847
	5.828×10^{-5}	2452	2.100	0.2595
13-cm bunch	5.993×10^{-5}	224	0.192	0.0252
	2.031×10^{-5}	694	0.594	0.0716

Table IV: Magnetic flux densities or Electric field required for the rf quadrupoles compensating for the 4-cm bunch.

Frequency	Magnetic flux gradient	Pole-tip flux density	Electric field gradient	Pole-tip E field	Pole-tip potential
f (GHz)	B_0' (T/m)	B_0 (T)	E_0' (MV/m^2)	E_0 (MV/m)	V_0 (MV)
0.680	1.48	0.0370	443	11.1	0.138
2.100	1.04	0.0259	311	7.78	0.097

gradient sampled by this particle is

$$\int_{-\ell/2}^{\ell/2} B'(t)dz' = \int_{-\ell/2}^{\ell/2} dz' B_0' \cos\left(\frac{\omega z'}{c} + \varphi + \frac{\omega z}{c}\right) = B_0'\ell \cos\left(\frac{\omega z}{c} + \varphi\right) \left\{\frac{\sin[\omega\ell/(2c)]}{\omega\ell/(2c)}\right\} . \tag{6.25}$$

The actual magnetic flux gradient has been diminished by the transit factor in the curly-bracketed term. Care must be taken in choosing the length of the quadrupole so that the transit factor will not be too small. If quadrupole lengths of $\ell = 10$ cm are used, the transit factors are 0.917 and 0.367, respectively, for frequencies 0.680 and 2.10 GHz. Take the 4-cm bunch as an example. If the rf quadrupoles for the two frequencies are placed at locations where the betatron function $\beta = 20$ m, the magnetic flux gradients are given by

$$B_0' \left\{\frac{\sin[\omega\ell/(2c)]}{\omega\ell/(2c)}\right\} = \frac{4\pi\Delta\nu_\beta(B\rho)}{\beta\ell} . \tag{6.26}$$

For the 50-GeV muons, the magnetic rigidity is $B\rho = 166.78$ T/m. The betatron tune is taken as $\nu_\beta \approx 6.24$. The maximum flux gradients B_0' and pole-tip flux densities B_0 are listed in the second and third columns of Table IV, where an aperture of $r_a = 2.5$ cm has been assumed for the quadrupoles. Obviously, iron-core quadrupoles cannot be used. Even air-core quadrupoles may not have the rise time that is fast enough at 2.1 GHz. One suggestion is to resort to electric quadrupoles rather than a magnetic one. However, electric quadrupoles will not be efficient in focusing an ultra-relativistic beam. Nevertheless, the equivalent electric field gradients are given by

$$E_0' = cB_0' . \tag{6.27}$$

The electric fields at the poles are $E_0 = E_0' r_a$ and the voltage at the poles are $V_0 = \frac{1}{2}E_0' r_a^2$. These are listed in the fourth, fifth, and sixth columns of Table IV.

Another possibility is to design cavities with resonating quadrupole modes. For example, the TM_{210} modes of cylindrical pill-box cavities will serve the purpose. The cavities, each of

width 10 cm, have radii

$$R = \frac{x_{21}c}{\omega_r} = 36.0 \text{ and } 11.7 \text{ cm} , \tag{6.28}$$

respectively, for the resonant frequencies $\omega_r/(2\pi) = 0.680$ and 2.10 GHz, where $x_{21} = 5.135$ is the first zero of the Bessel function of order 2. The longitudinal electric field is

$$E_z = E_0 J_2\left(\frac{x_{21}r}{R}\right)\cos 2\theta , \tag{6.29}$$

where θ is the azimuthal angle around the beam axis and the time dependency has been suppressed. The azimuthal magnetic flux density is

$$B_\theta = \frac{jE_0}{\omega_r} J_2'\left(\frac{x_{21}r}{R}\right)\frac{x_{21}}{R}\cos 2\theta , \tag{6.30}$$

where the factor j indicates that the magnetic flux density is 90° out of phase with the electric field. Thus, along the x-axis slightly offset from the center axis of the cavity,

$$B_y' \approx \frac{jE_0}{\omega_r}\frac{x_{21}^2}{R^2} , \tag{6.31}$$

and this must equal to the required electric field gradient E_0' given by Eq. (6.27) divided by c. The maximum longitudinal electric field is therefore given by

$$|E_0|\,[J_2]_{\max} = \frac{4c}{\omega_r}E_0'\,[J_2]_{\max} = \begin{cases} 59.9 \text{ MV/m} \\ 13.6 \text{ MV/m} \end{cases} , \tag{6.32}$$

for the two frequencies of 0.680 and 2.10 GHz, where use has been made of Eq. (6.28) and that fact that the Bessel function J_2 has a maximum of 0.482. These electric fields correspond to 2.47 and 0.342 Kilpatrick limits, respectively, for the cavity frequencies. Since the TM_{0n0} modes of the cavities are not to be used in BNS damping, they should be eliminated by absorbers or dampers so that no beamloading will result as the muon bunches are passing through them. Otherwise, a feed-forward scheme discussed in Sec. C. must be used so that transient beamloading can be eliminated.

VII. CONCLUSION

An impedance budget has been estimated for the 50GeV-50GeV muon collider ring. If a broadband impedance model is assumed, we find that, for such a collider ring, it will be hard to reduce $\mathcal{I}m\, Z_\parallel/n$ to below 0.5 Ω and $\mathcal{I}m\, Z_\perp$ to below 0.1 MΩ/m. The resonant angular frequency has been chosen to be $\omega_r = 50$ GHz, because it has been reported that $Z_\parallel/n$ does

not roll off up to even $f = 10$ GHz (or angular frequency 62 GHz) for the CERN LEP and the SLAC damping rings.

The phase-slip factor and its spread have been chosen to be 1×10^{-6} so that there will be negligibly small phase drifting during the lifetime of the muons. As a result, no bunching rf will be needed in the absence of coupling impedance. At the same time, any growth due to microwave instability can be made small.

Because of the high intensity of the bunches, potential-well distortion is extremely serious. This is compensated by using rf voltages so that their sum is equal and opposite to the wake potential of the bunch. However, these rf's can only compensate for potential-well distortion for a smooth bunch interacting with a smooth frequency dependent longitudinal impedance. Any imperfection in the bunch profile and deviation of the coupling impedance from a broadband will lead to accumulated growth in energy fluctuations. Since we are interested mostly in the first 1000 turns the muons made inside the collider ring, the actual accumulated growth depends very critically on the initial imperfection of the linear distribution of the bunch. If there is a way to smooth the linear distribution after ionization cooling and acceleration before injection into the collider ring, the accumulated growth for 1000 turns should be tolerable.

The compensating rf cavities cannot reduce the growth rate of microwave instability. However, they can lower the total microwave growth by reducing the ripples in the bunch and thus the seeds of the growth. In addition, the finite lifetime of the muons and the choice of the small slippage factor also help in making the microwave growth small and less important.

The beamloading voltages in these compensating cavities are found to be comparable to the wake-potential voltages they are supposed to cancel. A suggestion is to feed-forward via a tetrode an equal amount negative charge density onto the appropriate end of the cavity gaps so that the beamloading voltage will be cancelled.

Transverse microwave instabilities can be damped by chromaticities in both transverse planes. They can also be damped by installation of octupoles so that amplitude-dependent tune spread can be introduced.

Beam breakup is a severe issue for the muon bunches in the collider ring. If the growth is not too large, like that of the 13-cm bunch, it can be cured by introducing a tune spread in the bunch, either through chromaticity or amplitude dependency. The beam breakup is more serious for the 4-cm bunch because of its higher linear density. A pure tune spread may not be sufficient to cope with the problem and BNS damping is required. However, the actual implementation is nontrivial. This is because of the relative long bunch length. A

very fast pulsing (∼ns) rf quadrupole will be required. We find that cavities operating in the TM_{210} modes can be used for the compensation of the BNS tune shifts.

ACKNOWLEDGMENT

The author wishes to thank Professor J.S. Wurtele for a very fruitful discussion, and his careful reading of an earlier version of the manuscript.

References

[1] C.M. Ankenbrandt *et al.* (Muon Collider Collaboration), Phys. Rev. ST Accel. Beams **2**, 081001 (1999).

[2] K.Y. Ng, Part. Accel. **23**, 93 (1988).

[3] K.Y. Ng, *Impedances and collective instabilities of the Tevatron at Run II*, Fermilab Report FN-536, 1990.

[4] G. Sabbi (private communication).

[5] B. Zotter (private communication).

[6] E. Keil and W. Schnell, CERN/ISR-TH/69-48, 1969.

[7] K.Y. Ng, Nucl. Inst. Meth. **A404**, 199 (1998).

[8] E.-S. Kim, A,M, Sessler, and J.S. Wurtele, Phys. Rev. ST Accel. Beams 051001 (1999).

[9] G. Sabbi, *TRISIM User's Guide*, CERN Report CERN SL.94-73 (AP), 1994; G. Sabbi, *Simulation of Single-bunch Collective Effects in LEP by Linear Expansion of the Distribution Moments*, CERN Report CERN SL/95-25 (AP), 1995.

[10] G. Jackson, Proc. 1995 Part. Accel. Conf. and Int. Conf. High-Energy Accel. May 1-5, 1995, Dallas, Texas, Ed. L. Gennari, p. 2931.

[11] P. Colestock (private communication).

[12] W.D. Kilpatrick, *Criterion for Vacuum Sparking Designed to Include Both RF and DC*, LBL Report 2321, 1953.

[13] J.E. Griffin, *RF System Considerations for a Muon Collider Proton Driver Synchrotrons*, Fermilab report FN-669, 1998.

[14] B. Zotter, Proc. First Course Int. School Part. Accel., Erice, Nov. 10-22, 1976, p. 176.

[15] A.W. Chao, *Physics of Collective Beam Instabilities in High Energy Accelerators*, John Wiley & Sons, Inc., 1993, p. 70.

[16] E.-S. Kim, A,M, Sessler, and J.S. Wurtele, Part. Accel. Conf., March 29 - April 2, 1999, New York City, Article THP45.

[17] V. Balakin, A. Novokhatsky, and V. Smirnov, Proc. 12th Int. Conf. High Energy Accel., Fermilab 1983, p 119.